Studies by the U.S. Geological Survey in Alaska, 2000
U.S. Geological Survey Professional Paper 1662

Mount Griggs: A Compositionally Distinctive Quaternary Stratovolcano Behind the Main Volcanic Line in Katmai National Park

By Wes Hildreth, Judy Fierstein, Marvin A. Lanphere, *and* David F. Siems

Abstract

Mount Griggs, the highest peak in Katmai National Park, is a fumarolically active andesitic stratovolcano that stands alone 12 km behind the main volcanic chain of the Alaska Peninsula range crest. K-Ar ages indicate that the volcano is as old as 292±11 ka and thus predates inception of the nearby volcanic-front centers. The middle Pleistocene edifice was glacially ravaged before construction of the well-preserved modern cone during the late Pleistocene and Holocene. Collapse of the southwest sector early in the Holocene left a 1.5-km-wide amphitheater at the summit and shed a 1-km^3-volume debris avalanche into the valley of Knife Creek. Smaller debris-avalanche deposits later emplaced to the east, north, and west are also of early Holocene age. Postcollapse andesite eruptions built an inner cone that nearly filled the amphitheater and covered the southwest slope of the volcano with a fan of leveed lava flows. The inner cone is topped by a pair of nested craters and supports clusters of mildly superheated, sulfur-precipitating fumaroles. Present-day edifice volume is approximately 20 to 25 km^3, of which about 2.2 km^3 was erupted during the Holocene. Average productivity is estimated to have been at least 0.12 km^3/k.y. for the lifetime of the volcano and appears to have been in the range 0.2–0.4 km^3/k.y. since about 50 ka. Eruptive products are olivine-bearing two-pyroxene andesites rich in plagioclase that have remained especially phenocryst rich throughout the history of the volcano. A total of 77 analyzed samples define a typical Ti-poor, medium-K calc-alkaline arc suite, largely ranging in SiO_2 content from 55 to 63 weight percent, that shows little systematic change over time. Relative to products of the nearby volcanic-front centers, those of Mount Griggs are slightly depleted in Fe, generally enriched in Rb, Sr, Al, and P, and consistently enriched in K and Zr; its fumarolic gases are notably richer in He. The magmatic plumbing system of Mount Griggs is independent of those beneath the main volcanic chain, probably all the way to mantle depths. Holocene ash from Mount Griggs is inconspicuous beyond the edifice, and no evidence was found for particularly explosive ejection of its crystal-rich andesitic magmas. Future debris flows from any sector of the volcano would have a 25-km runout into Naknek Lake through uninhabited wilderness.

Introduction

The Quaternary volcanic chain of Katmai National Park is the most tightly spaced line of stratovolcanoes in Alaska (fig. 1). Along the volcanic front, crater-to-crater spacing between adjacent (commonly contiguous) edifices is typically 5 km or less. A subset of these edifices at the head of the Valley of Ten Thousand Smokes is the Katmai cluster, made up of numerous stratocones and associated lava domes (Hildreth, 1987; Hildreth and Fierstein, 2000). Of the many discrete Quaternary volcanic vents in the Katmai cluster, only Mount Griggs, the subject of this chapter, lies significantly off axis, some 12 km behind (northwest of) the main volcanic line (fig. 1).

Mount Griggs is one of the larger and better preserved stratovolcanoes in the region, rising about 1,750 m above the floor of the Valley of Ten Thousand Smokes (fig. 2). With its summit reaching about 7,650 ft (2,330 m) in elevation, Mount Griggs is the highest peak in Katmai National Park. Present-day symmetry of the apparently little-dissected edifice (fig. 2) reflects numerous effusions of andesitic lava during the late Pleistocene and Holocene that have healed and concealed older scars of glacial erosion. Moderately productive during postglacial time and still fumarolically active, Mount Griggs is also the longest lived center in the Katmai cluster; its construction began nearly 300 ka. Although the volcano has not erupted historically, a large volume of Holocene lava covers its southwest slope (figs. 2, 3).

The main volcanic chain from Snowy to Alagogshak (fig. 1) is constructed along the preexisting range crest (Pacific-Bristol Bay drainage divide), where the rugged prevolcanic basement typically reaches 4,000 to 5,500 ft

(1,200–1,675 m) in elevation. Because the line of volcanic summits reaches 6,000 to 7,100 ft (1,830–2,165 m) in elevation and lies in a region of high precipitation, all the range-crest centers are extensively ice covered. Although Mount Griggs is higher still, its position 12 km northwest of the frontal axis receives less precipitation, resulting in less glacial ice on the edifice. Five narrow ice tongues (fig. 4) descend from shallow cirques high on the north slopes to termini at 3,000- to 3,800-ft (915–1,160 m) elevation, and a sixth extends down the south slope from the summit icefield to a terminus at 5,500-ft (1,675 m) elevation (see figs. 2, 4–7).

All the streams draining Mount Griggs are tributaries of either Ikagluik Creek or the Knife Creek branch of the Ukak River (fig. 3). These streams flow northward and nearly meet just before entering the Iliuk Arm of Naknek Lake (fig. 1). Debris flows resulting from eruptions or avalanches at Mount Griggs would therefore be expected to affect drainage systems only to the north and northwest, not those of the Pacific slope.

Mount Griggs lies in uninhabited national-park wilderness. The base of the volcano is a 1-day hike from the hill west of Three Forks (fig. 3), which is in turn accessible in summer months by dirt road from Brooks Camp (fig. 1). Many aircraft—cargo, passenger, and sightseeing—commonly overfly the volcano, but only a handful of the 100-odd backpackers who roam the Valley of Ten Thousand Smokes each summer ever venture onto the slopes of Mount Griggs.

Earlier Work

Little fieldwork has previously been undertaken at Mount Griggs. The National Geographic Society expeditions of 1915–19 led by Robert Fiske Griggs (1881–1962) identified the mountain as a volcano on the topographic map they prepared of the Katmai region, and the first photographs of Mount Griggs (then known as Knife Peak) are in their publications (Griggs, 1922; Allen and Zies, 1923), but no mention of its lavas, structure, or fumaroles appears in their reports. Charles Yori climbed the mountain alone on August 20, 1923, photographed the summit icefield, and took an ande-

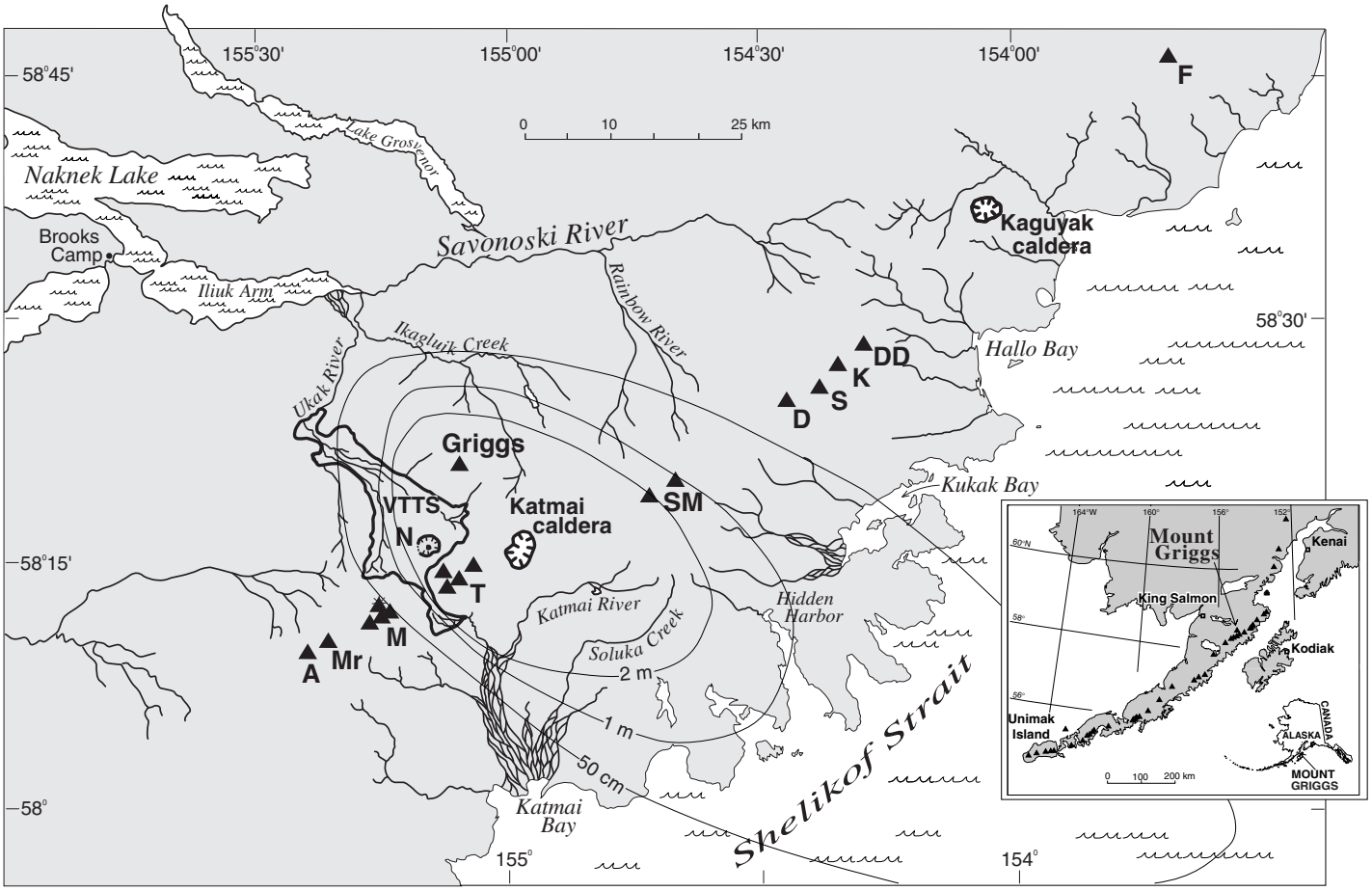

Figure 1. Southern Alaska, showing location of Mount Griggs stratovolcano about 12 km behind late Quaternary volcanic axis, which straddles drainage divide along this stretch of the Alaska Peninsula. Triangles indicate andesite-dacite stratovolcanoes, identified by letter: A, Alagogshak; D, Denison; DD, Devils Desk; F, Fourpeaked; K, Kukak; M, Mageik (cluster of four); Mr, Martin; S, Steller; SM, Snowy Mountain (two cones); T, Trident (cluster of four). VTTS, the Valley of Ten Thousand Smokes ash-flow sheet (outlined area), which erupted at Novarupta (N) in June 1912. Isopachs show thickness of cumulative 1912 plinian fallout, originally 2 to 5 m thick across Mount Griggs. Were pyroclastic flows or debris flows to originate at Mount Griggs itself, they would be confined to Ikagluik Creek or the VTTS, both of which drain to the Iliuk Arm of Naknek Lake.

site sample (later analyzed by C.N. Fenner) from an outcrop "about 100 feet below summit" (Fenner, 1926, p. 684). To the best of our knowledge, the fumaroles high on the volcano were first mentioned by Muller and others (1954).

In 1959, Professor Griggs received a letter from the president of the National Geographic Society informing him that the U.S. Board of Geographic Names was changing the name of Knife Peak to Mount Griggs (Higbie, 1975). In 1963, the ashes of Griggs and his wife joined volcanic ash from the 1912 eruption of Novarupta scattered on the airy summit of the volcano.

Kosco (1980) joined our field party in 1976 and produced some chemical and petrographic data for Mount Griggs lavas. Hildreth (1987) and Wes Hildreth (in Wood and Kienle, 1990) composed short summaries of what was then known about the volcano. A more inclusive summary was given by Hildreth and Fierstein (2000), but in this chapter, based on helicopter-supported fieldwork in 1997–99, we document the present state of our knowledge of Mount Griggs. Although our study is a moderately detailed field reconnaissance, better understanding of the eruptive and erosional history of Mount Griggs could certainly be achieved by means of additional fieldwork and radiometric dating. The 1912 fallout that so thickly mantles the young southwest sector of the cone (fig. 2) makes it difficult to find organic material, the dating of which might help unravel the emplacement history of the Holocene lava apron.

Basement Rocks

The volcanic edifice of Mount Griggs has been constructed upon a set of glaciated ridges carved from subhorizontal marine siltstone and sandstone of the Jurassic Naknek Formation (Riehle and others, 1993; Detterman and others, 1996). These stratified rocks are intruded locally by several porphyritic granitoid stocks of Tertiary age, one of which is abutted by Mount Griggs lavas on the northwest side of the volcano (fig. 4). Although Mount Griggs lavas descend to as low as 1,900-ft (580 m) elevation to the north and southwest

Figure 2. Oblique aerial photograph of Mount Griggs stratovolcano. Right (southeast) half of visible edifice, including 7,650-ft (2,332 m)-elevation summit, consists largely of late Pleistocene lava flows; left (southwest) slope and amphitheater-filling black inner cone consist principally of Holocene lava flows and proximal agglutinate. Massive exposure at far-left base of cone is debris-avalanche deposit (unit dk) as much as 200 m thick. Two windows of middle Pleistocene lava flows are designated by their ages, 133 and 160 ka. At foot of cone in foreground, remnants of a late Pleistocene scoria flow from Mount Katmai (unit sf; see fig. 10) form rims of gulches cut into all-andesite diamict (unit ds). Knife Creek tributary streams bounding volcano are the Griggs Fork (right) and the Juhle Fork (left). Beyond the Juhle Fork is Mount Juhle, which consists largely of Jurassic marine sedimentary strata of the Naknek Formation, intruded by a Tertiary porphyritic granitoid pluton (see fig. 4). Broken Mountain (lower left), Knife Creek valley (part of the Valley of Ten Thousand Smokes), and glacier (lower right) are covered by pyroclastic-flow and fall deposits from 1912 eruption of Novarupta (out of view, slightly behind and to left). Pale-gray mantle draping Mount Griggs is 1912 dacitic pumice-fall deposit, which on lower slopes rests also on thin pink run-up sheets of 1912 rhyolitic ignimbrite. View northward across upper Knife Creek.

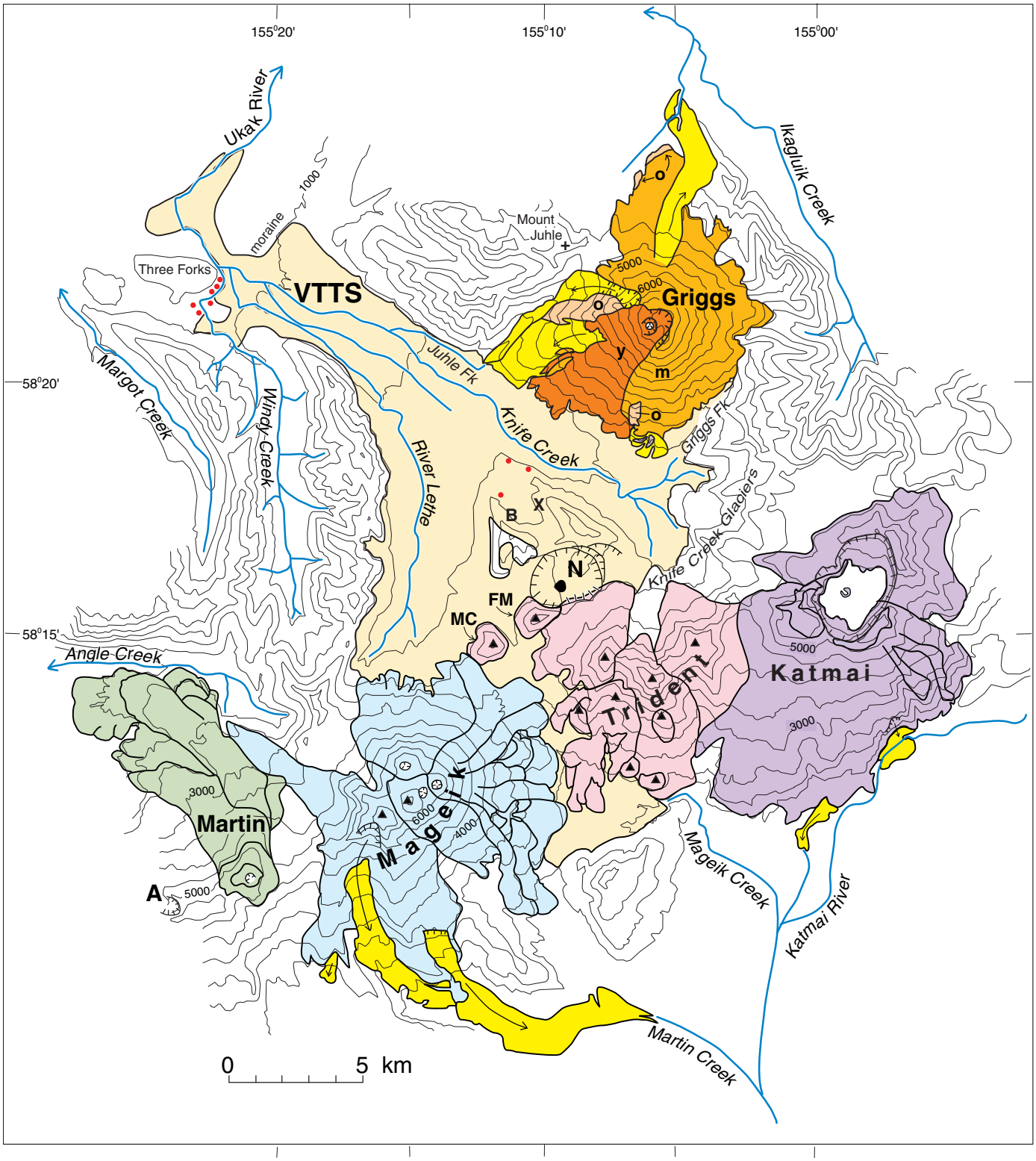

Figure 3. Topographic map of Mount Griggs and vicinity, showing main drainages, nearby volcanoes, and places mentioned in text. A, Alagogshak Volcano; B, Baked Mountain; FM, Falling Mountain dome; MC, Mount Cerberus dome; N, Novarupta dome; X, Broken Mountain. On Mount Griggs: o, m, y, oldest, middle, and youngest lavas, respectively, as discussed in text; glaciers are omitted for clarity. Bright yellow areas, debris-avalanche deposits. Red dots, remnants of Knife Peak debris-avalanche deposit beyond limits of Mount Griggs edifice itself. Pale-tan valley fill is 1912 ignimbrite in the Valley of Ten Thousand Smokes (VTTS). Near Three Forks in lower VTTS is valley-crossing Neoglacial moraine discussed in text (see Hildreth, 1983; Fierstein and Hildreth, 1992). For geology of volcanoes on main volcanic line, see Hildreth and Fierstein (2000).

(fig. 4), basement rocks crop out at as high as 4,400-ft (1,340 m) elevation at the northwestern and eastern margins of the cone, attesting to the rugged prevolcanic relief draped by the volcanic pile.

Although Permian to Jurassic sedimentary rocks that regionally underlie the Naknek Formation (itself 2 km thick) do not crop out in the Katmai area, the stratigraphic framework of the Alaska Peninsula (Detterman and others, 1996) suggests that such rocks are as much as 3.5 km thick beneath Mount Griggs.

A few remnants of Pliocene or early Quaternary volcanic rocks cap peaks and ridges near Mount Griggs (fig. 4), but most such rocks (more extensive farther eastward; see Riehle and others, 1993) have been eroded from the study area (fig. 1).

Compound Edifice

The apparent symmetry of the andesitic stratovolcano as viewed from the Valley of Ten Thousand Smokes (fig. 2) belies a complex history that is partly revealed by its three concentric summit craters. The outer rim defines a 1.5-km-wide amphitheater that is open to the west but is largely filled by a postglacial andesite cone topped by a nested pair of inner craters. The amphitheater apparently formed by sector collapse during the early Holocene, when the largest of several debris-avalanche deposits was emplaced. The edifice now exposed thus consists of several components of different ages, which are described below within the following framework: (1) three windows of severely eroded lavas of middle Pleistocene age; (2) the main late Pleistocene cone, only lightly eroded, and its amphitheater-forming debris-avalanche deposit; and (3) the Holocene inner cone that filled the amphitheater and created the southwesterly apron of leveed lava flows, virtually uneroded.

Middle Pleistocene Exposures

The oldest lavas exposed at Mount Griggs are two or more flows of plagioclase-rich pyroxene andesite (60 weight percent SiO_2) that form 150-m-high cliffs along the Juhle Fork of Ikagluik Creek at the north foot of the volcano (fig. 4). These distal, devitrified to partly glassy lava flows rest on Jurassic basement and are overlain by a sheet of till that obscures their contact with younger Mount Griggs lavas. The two noncontiguous cliff exposures are formed by discrete lava flows that are similar in thickness, petrography, and composition (samples 2294, 2309, table 1), yet differ significantly from the more mafic lava flows that crop out a few hundred meters southwest. The more easterly lava of the pair yielded a whole-rock K-Ar age of 292±11 ka (table 2) and so is the earliest eruptive product recognized at Mount Griggs.

A second exposure of glacially eroded middle Pleistocene lava flows forms the ridge that rims the south wall of the Juhle Fork of Knife Creek and culminates in a craggy shoulder at 6,200-ft (1,890 m) elevation about 2 km west of the summit (figs. 2–4, 6). The crags are eroded from four or five slabby flows of flow-foliated silicic andesite (59–62 weight percent SiO_2) that dip about 20º W. and thicken downslope to the west, each to 25 to 40 m thick. They are underlain by a stack of several thinner (10–20 m thick) flows of more mafic andesite (56 weight percent SiO_2) marked by oxidized rubbly zones that forms the 600-m-high wall which extends downward to the glacier flooring the upper Juhle Fork. The topmost flow capping the highest crag gave a whole-rock K-Ar age of 160±8 ka (fig. 4; table 2).

The third window of glaciated lavas that unequivocally predates construction of the main late Pleistocene cone crops out at 2,500- to 3,500-ft (760–1,065 m) elevation near the south base of the volcanic edifice (figs. 2, 4, 6). The 400- by 750-m-wide, reddish-brown-weathering exposure stands out as a glacially smoothed bulge that branches downslope into a pair of steep rubbly spurs. At least five andesitic lava flows (56–58 weight percent SiO_2) are present, but neither the base nor the top of the stack is exposed. Gray-brown to pale-purple massive zones support 8- to 15-m-high benches that are separated by oxidized flow-breccia zones, some of which are tens of meters thick. The toe of the stack is concealed by thick scree and alluvium (dominantly reworked 1912 pumice), and the top is covered by wind-deflated diamicton—either till or avalanche rubble—armored by a lag of varied andesite blocks. A flow midway through the stack, third from the bottom, yielded a whole-rock K-Ar age of 133±25 ka (fig. 4; table 2).

Locally mantling the east rim of this southerly window of older lavas is a 25-m-wide remnant of a black scoria deposit (53 weight percent SiO_2), only 1 m thick. Contained in a fines-poor matrix dominated by coarse crystal ash, most scoria is smaller than 1 cm across, and the largest is only 4 cm across. Much of the deposit is poorly sorted, unstratified, and infiltrates the rough rubbly surface of the underlying lava, but the undisturbed top 20 cm looks like primary fallout. The remnant is lithic poor and locally indurated by orange secondary minerals. The scoria is notably lower in K and Zr contents than the array of eruptive products at Mount Griggs, but in its composition it closely matches the suite erupted at nearby Mount Katmai.

Late Pleistocene Outer Cone

After glacial destruction of the volcanic edifice(s) from which the lavas of the older windows just described were erupted, late Pleistocene activity sufficiently outpaced erosion to permit accumulation of a fairly symmetrical cone, about 8 km across and 1.5 km high. Much of that cone remains conspicuous today, somewhat degraded but little dissected (fig. 2). Its south and east slopes are near-primary concave surfaces (fig. 2), its north half is shallowly incised by five narrow ice tongues (fig. 4), and its southwesterly quadrant was destroyed by sector collapse during the early Holocene. No flank vents have been recognized, and all the flows exposed appear to be summit derived, cut off from a slightly higher former source

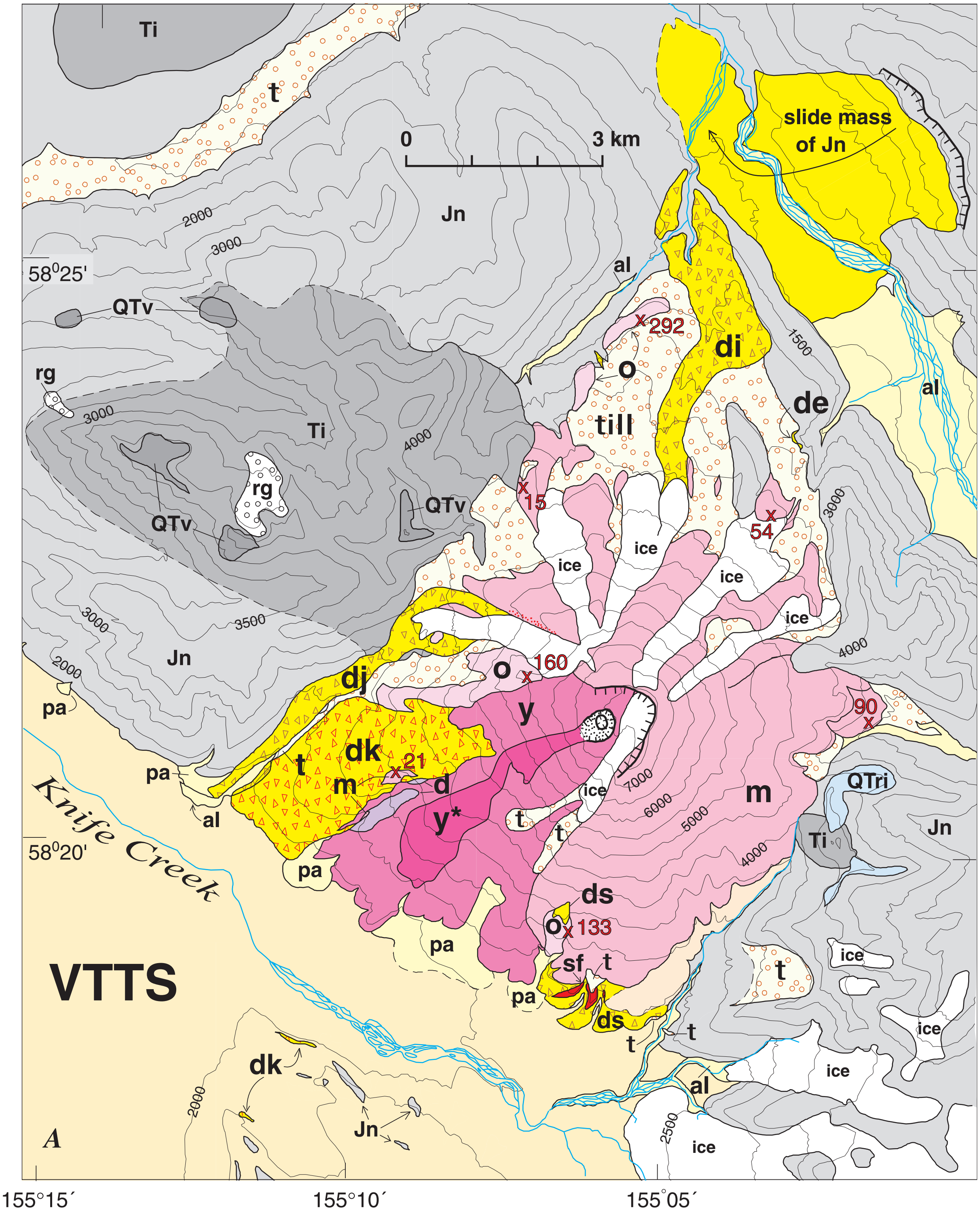

Figure 4. Reconnaissance geologic map of Mount Griggs area, southern Alaska (fig. 1). Topography simplified from U.S. Geological Survey 1:63,360-scale Mount Katmai B–4 quadrangle; contour interval, 500 ft. *A*, Geologic units. Pale-tan unit in the Valley of Ten Thousand Smokes (VTTS) is ignimbrite from 1912 eruption of Novarupta. On Mount Griggs edifice: d, dacite lava flow; m, late Pleistocene andesite cone; o, old andesite windows (middle Pleistocene); y, post-collapse Holocene andesite cone and lava fan; y*, youngest set of andesitic lava flows. Mass-flow deposits (bright yellow): de, diamict of Ikagluik Creek; di, Ikagluik Creek debris-avalanche deposit; dj, Juhle Fork debris avalanche; dk, Knife Peak debris avalanche; ds, diamict of Griggs Fork. Surficial deposits: al, alluvium; pa, pumiceous alluvial fans of remobilized 1912 fallout; rg, rock glaciers; sf (red), late Pleistocene dacitic scoria flow from Mount Katmai; t, glacial till. Basement rocks: Jn, Jurassic Naknek Formation, subhorizontal marine siltstone and sandstone; QTri, rhyolitic

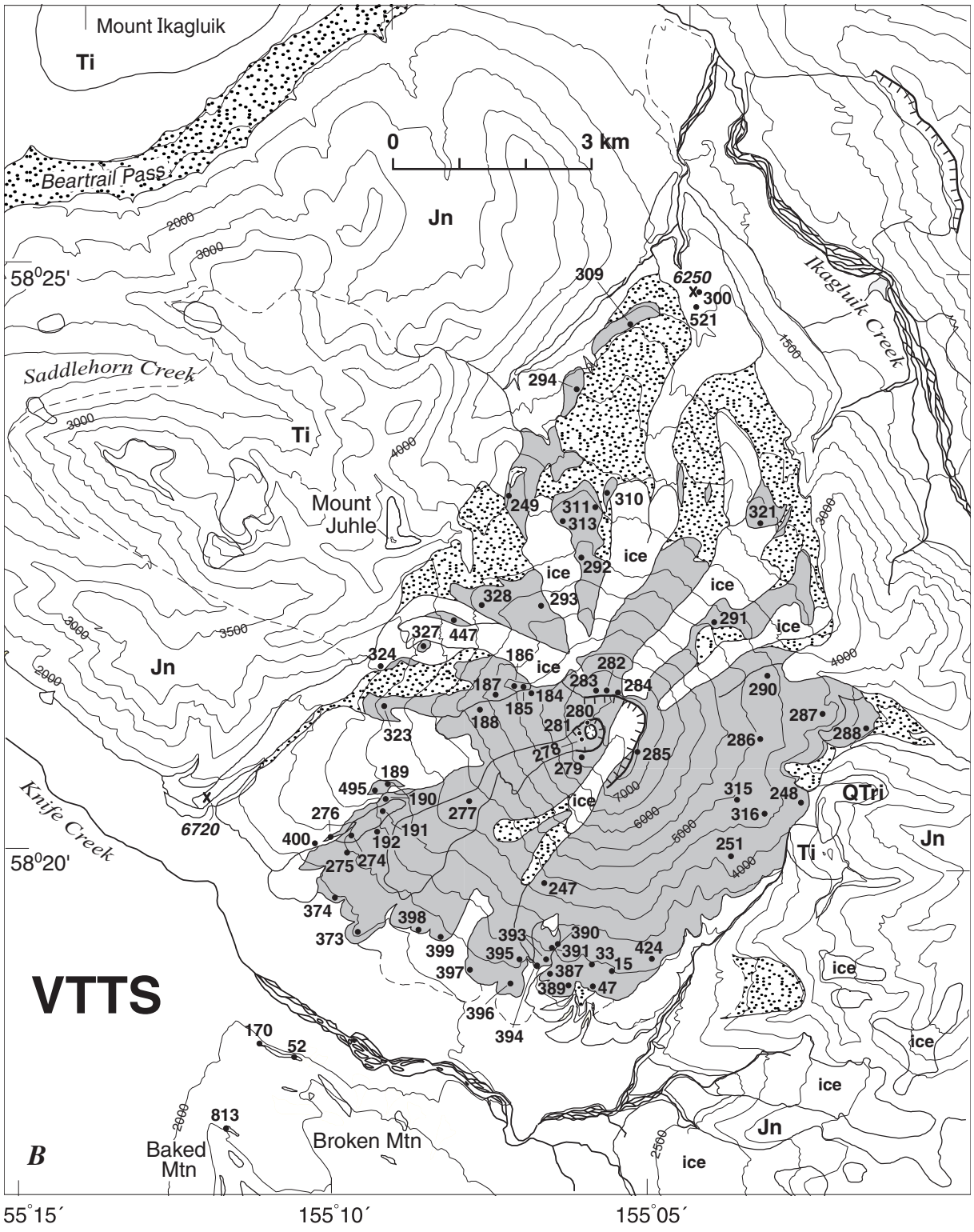

ignimbrite, undated; QTv, basaltic, andesitic, and dacitic lava remnants, mostly Pliocene, northwest of Mount Griggs; Ti, Tertiary porphyritic granitoid intrusions. Red stippling along northern margin of northwestern glacier denotes hydrothermally altered zone at source of Juhle Fork debris-avalanche deposit. Red X's, sample sites for K-Ar ages listed in table 2; adjacent numbers give ages (in thousands of years). At south-central edge, two ignimbrite-mantled ridges defined by 2,500-ft contour are noses of Baked and Broken Mountains (see fig. 3), where blocks of avalanche-deposited andesite of Mount Griggs overlie basement rocks in scattered windows. *B*, Placenames and sample locations. All samples listed in table 1 are indicated except those from avalanche blocks 2350–A, 2350–B, and 2352, which are in the Windy Creek embayment of the Valley of Ten Thousand Smokes. x6250 and x6720, sites of two radiocarbon-dated samples atop debris-avalanche deposits, as discussed in text. Same base as in figure 4*A*.

Table 1. Chemical analyses of eruptive products from Mount Griggs, Alaska.

[Major-oxide contents in weight percent, normalized to H_2O-free totals of 99.6 weight percent (allowing 0.4 weight percent for trace oxides and halogens), determined by wavelength-dispersive X-ray-fluorescence analysis in the U.S. Geological Survey laboratory at Lakewood, Colo.; analyst, D.F. Siems. Rb, Sr, and Zr contents in parts per million, determined by energy-dispersive X-ray-fluorescence analysis; analyst, D.F. Siems. Precision and accuracy were discussed by Bacon and Druitt (1988). FeO*, total Fe calculated as FeO. LOI, weight loss on ignition at 900°C. Original total, volatile-free sum of 10 major-oxide analyses before normalization, with total Fe calculated as Fe_2O_3]

Sample	SiO_2	TiO_2	Al_2O_3	FeO*	MnO	MgO	CaO	Na_2O	K_2O	P_2O_5	LOI	Original total	Rb	Sr	Zr
Inner cone															
2184	57.5	0.86	17.59	7.13	0.14	3.80	7.38	3.70	1.26	0.23	0.09	99.41	24	384	140
2188	57.4	.88	17.71	7.16	.14	3.66	7.16	3.87	1.31	.28	.14	99.27	23	371	140
2190	57.3	.88	17.64	7.28	.14	3.76	7.42	3.65	1.27	.24	–.06	98.86	21	374	137
2192	59.1	.81	17.45	6.79	.14	3.15	6.53	3.84	1.54	.23	.16	99.21	28	357	162
2275	58.7	.81	17.61	6.76	.14	3.20	6.66	3.90	1.52	.26	.29	99.04	32	362	154
2276	57.4	.86	17.64	7.21	.14	3.73	7.36	3.69	1.29	.25	–.05	99.32	25	392	145
2277	57.2	.87	17.65	7.33	.14	3.83	7.45	3.61	1.26	.23	–.06	99.23	20	390	141
2278	60.2	.81	17.19	6.36	.13	2.88	6.20	3.93	1.64	.22	–.03	98.96	34	348	171
2279	55.1	.89	18.48	7.55	.15	4.32	8.32	3.50	1.03	.23	.38	98.38	18	371	122
2280	59.3	.83	17.56	6.73	.13	3.07	6.38	3.84	1.48	.24	.54	98.20	29	367	169
2281	60.4	.78	17.22	6.27	.13	2.84	6.13	3.91	1.65	.22	.66	98.55	33	347	157
2373	61.0	.75	17.05	6.22	.13	2.70	5.89	3.93	1.74	.23	.25	98.36	29	333	179
2374	59.6	.79	17.41	6.56	.14	2.95	6.38	3.92	1.59	.23	.16	98.96	33	346	167
2395	56.9	.86	17.90	7.22	.14	3.82	7.47	3.79	1.27	.27	.01	99.22	24	360	137
2396	58.7	.84	17.60	6.82	.14	3.19	6.69	3.86	1.49	.22	.15	99.45	31	342	161
2397	55.9	.87	18.17	7.38	.14	4.11	7.93	3.68	1.14	.23	–.04	99.08	24	367	127
2398	60.7	.76	17.12	6.30	.13	2.75	5.98	3.90	1.72	.22	.00	98.85	35	345	176
2399	61.9	.74	16.72	6.04	.13	2.50	5.49	3.91	1.90	.22	.21	98.86	40	328	190
Outer cone															
47	55.7	0.90	18.50	7.82	0.16	3.81	7.53	3.87	1.10	0.21	0.25	99.59	20	432	142
2189	56.3	.89	18.38	7.69	.15	3.70	7.28	3.82	1.15	.24	–.04	99.06	27	429	140
2191	63.0	.69	16.53	5.52	.12	2.30	5.19	3.97	2.04	.23	.29	98.95	41	328	204
2247	59.2	.75	17.51	6.36	.13	3.39	6.76	3.74	1.55	.23	.26	99.02	30	361	151
2248	59.3	.81	17.55	7.04	.15	2.85	6.10	4.10	1.45	.25	.01	99.07	28	403	164
2249	57.9	.76	17.84	6.68	.14	3.81	7.21	3.69	1.32	.21	–.09	99.34	28	400	139
2251	60.1	.82	17.44	6.50	.14	2.68	5.81	4.22	1.61	.26	.09	99.06	33	382	178
2274	57.6	.75	18.07	6.71	.14	3.78	7.38	3.59	1.33	.24	.29	99.36	28	415	137
2274–A	63.4	.67	16.52	5.39	.12	2.16	5.01	3.97	2.09	.22	.44	98.87	43	315	203
2282	55.1	.85	17.86	7.93	.15	5.00	8.15	3.20	1.15	.21	.88	98.41	26	336	112
2283	55.2	.89	18.96	7.83	.14	4.30	7.79	3.25	1.03	.20	2.04	96.72	20	339	114
2284	58.0	.85	18.01	7.29	.15	3.26	6.57	3.93	1.28	.26	.36	98.69	28	417	147
2285	55.5	.86	18.18	7.64	.14	4.10	8.44	3.34	1.12	.22	.00	98.58	22	383	114
2286	59.8	.80	17.41	6.78	.14	2.89	5.92	4.06	1.55	.27	.10	99.02	33	395	168
2287	60.3	.77	18.10	5.67	.13	2.50	5.90	4.39	1.58	.26	.23	98.89	32	380	169
2288	62.7	.69	17.98	4.54	.12	1.59	5.10	4.70	1.88	.26	.35	98.65	43	370	205
2290	59.0	.79	18.04	6.14	.13	3.18	6.46	4.16	1.42	.27	.06	99.02	32	389	157
2291	59.1	.82	17.54	7.05	.14	3.12	6.16	4.00	1.46	.24	.16	98.92	30	383	162
2292	57.1	.76	17.44	7.22	.15	4.20	7.70	3.57	1.23	.24	.00	99.39	27	369	132
2293	60.2	.72	17.43	6.15	.14	3.18	6.06	3.82	1.68	.23	1.06	97.34	40	351	165
2310	58.6	.78	17.64	7.17	.15	3.29	6.57	3.88	1.32	.24	.18	98.65	27	386	129
2311	57.2	.76	17.29	7.23	.15	4.36	7.60	3.55	1.24	.25	–.04	99.24	28	363	135
2313	57.1	.75	17.27	7.26	.15	4.41	7.61	3.52	1.24	.24	.11	99.07	26	360	130
2315	59.1	.81	17.51	7.12	.15	2.94	6.07	4.15	1.46	.29	.17	99.32	35	414	158
2316	59.3	.81	17.54	7.02	.15	2.86	6.10	4.07	1.45	.25	–.03	99.23	28	391	152
2321	57.3	.81	17.67	7.12	.14	3.91	7.41	3.62	1.35	.22	–.14	99.10	30	346	140
2328	59.8	.73	17.46	6.24	.14	3.21	6.42	3.80	1.62	.24	.57	98.32	38	360	158
2387	57.8	.86	18.03	7.26	.15	3.31	6.67	3.94	1.33	.26	–.04	98.84	26	415	154
2389	56.9	.81	17.76	7.39	.14	3.78	7.77	3.52	1.27	.22	.10	99.90	28	400	136
2424	54.9	.81	17.63	7.61	.14	5.12	8.92	3.22	1.05	.21	–.05	99.24	22	367	109
2495	57.2	.87	18.29	7.45	.15	3.48	6.81	3.86	1.25	.24	.34	98.86	22	409	144
KNM–15	62.5	.71	16.86	5.70	.12	2.32	5.53	3.84	1.86	.16	.25	98.65	38	330	189
KNM–33	55.5	.88	18.15	7.51	.14	4.18	8.15	3.78	1.09	.17	.28	99.34	19	364	133
Old windows															
2185	61.9	0.63	17.14	5.72	0.14	2.45	5.51	4.12	1.71	0.25	0.06	99.20	36	365	151
2186	59.0	.72	17.59	6.44	.14	3.43	6.84	3.78	1.44	.23	–.07	99.10	28	404	137
2187	55.2	.81	18.11	7.55	.15	4.50	8.75	3.27	1.06	.16	–.06	99.54	18	379	106
2294	60.1	.68	17.44	6.15	.14	3.11	6.33	3.92	1.55	.23	.09	99.04	33	377	146
2309	60.1	.72	17.50	6.52	.15	2.86	6.03	4.02	1.46	.22	.15	98.87	29	373	131
2323	57.0	.77	18.09	6.85	.14	4.02	7.63	3.56	1.30	.25	–.12	99.01	22	428	130
2327	57.8	.75	17.66	6.98	.14	3.96	7.29	3.63	1.13	.24	.00	98.61	23	429	114
2390	57.8	.75	17.91	6.87	.15	3.62	7.47	3.60	1.24	.22	–.06	98.89	21	418	122
2391	56.2	.88	18.23	7.86	.16	3.83	7.21	3.85	1.08	.28	.02	98.86	20	428	144
2393	58.2	.74	17.80	6.73	.14	3.49	7.25	3.70	1.30	.27	.10	99.14	24	422	127
2394	58.1	.74	17.96	6.74	.14	3.44	7.26	3.69	1.27	.21	.00	98.99	26	431	128
2447	59.2	.77	17.19	6.94	.15	3.59	6.47	3.82	1.30	.20	.11	98.70	23	368	122
2447A	50.9	.90	19.27	8.48	.15	6.31	1.04	2.70	.67	.14	.77	98.36	10	478	78

Table 1. Chemical analyses of eruptive products from Mount Griggs, Alaska—Continued.

Sample	SiO_2	TiO_2	Al_2O_3	FeO*	MnO	MgO	CaO	Na_2O	K_2O	P_2O_5	LOI	Original total	Rb	Sr	Zr
Avalanche blocks															
52	59.6	0.67	17.42	6.25	0.13	3.44	6.54	3.85	1.48	0.18	0.38	98.36	33	339	169
170	57.0	.75	17.27	7.21	.14	4.29	8.03	3.53	1.20	.19	< .01	99.79	23	371	138
813	57.4	.66	18.25	6.23	.13	3.82	7.96	3.63	1.33	.15	< .01	100.42	24	352	141
813i	53.6	.79	18.38	7.57	.14	5.54	9.38	3.09	.93	.14	< .01	100.27	13	349	109
2300	60.2	.76	17.35	6.60	.14	3.00	6.04	3.84	1.49	.22	.47	98.75	29	344	151
2324–A	55.5	.84	17.76	7.65	.15	4.85	8.12	3.32	1.19	.20	–.04	98.76	24	352	121
2350–A	59.1	.71	17.28	6.63	.15	3.48	6.64	3.95	1.44	.27	.02	98.61	32	375	153
2350–B	57.5	.74	17.28	7.00	.15	4.51	7.14	3.74	1.29	.24	–.13	99.01	26	353	141
2352	56.5	.76	17.07	7.31	.15	4.86	7.95	3.53	1.19	.25	.35	98.35	20	361	128
2400A	55.9	.86	18.32	7.83	.14	3.96	8.24	3.11	1.00	.19	.76	98.51	22	396	120
2400B	58.5	.75	17.32	6.92	.15	3.76	7.01	3.67	1.35	.18	1.01	97.86	26	373	144
2521A	59.2	.67	16.88	6.37	.15	4.41	6.68	3.62	1.43	.20	.41	98.52	33	337	138
2521i	53.9	.81	17.50	7.77	.16	6.93	8.53	3.04	.84	.11	.35	98.49	11	350	94

Table 2. Whole-rock K-Ar ages and analytical data for Mount Griggs samples.

[Analysts: K, D.F. Siems; Ar, F.S. McFarland and J.Y. Saburomaru. Constants: λ=0.581×10^{-10} yr^{-1}; λ_β=4.962×10^{-10} yr^{-1}; $^{40}K/K$=1.167×10^{-4} mol/mol]

Sample	Location (fig. 4)	Weight percent		Radiogenic ^{40}Ar		Calculated age (ka)
		SiO_2	K_2O	10^{-13} mol/g	percent	
K–2186	Crag at 6,200+-ft elevation on WNW. shoulder. Top flow of old glaciated stack.	59.0	1.552±0.004	3.581	15.1	160±8
K–2189	West slope. Top flow on N rim of gorge at 3,400-ft elevation, 200 m E. of hill at 3,500+-ft elevation. Overlain directly by unit dk.	56.3	1.197±0.003	.3694	1.4	21±11
K–2249	Northern distal lava flow. Thick ice-scoured flow on 4100-ft ridge atop basement rocks, 400 m N. of hill at 4,230-ft elevation.	57.9	1.384±0.001	.2914	.3	15±18
K–2288	Eastern basal distal lava flow. Intracanyon flow, 150 m thick, in fork of Ikagluik Creek.	62.7	2.027±0.006	2.644	11.4	90±7
K–2309	Northern basal distal lava flow on 2,500-ft rim of canyon tributary to Ikagluik Creek.	60.1	1.515±0.002	6.357	14.8	292±11
K–2321	Northeastern basal distal lava flow, 80 m thick, on 3,200-ft N. rim of gorge above glacier snout; 350 m S of map location x3060.	57.3	1.479±0.001	1.143	5.4	54±8
K–2390	South window, 3.5 km S. of summit crater. Middle flow of old stack at 3,000-ft elevation.	59.0	1.254±0.001	2.395	2.6	133±25
K–2274A	Convolutely foliated dacite lava flow at 2,400- to 3,500-ft elevation, W. slope.	63.4	2.09	0	0	no age (failed twice)

vent by the present-day rim of the amphitheater (fig. 5). A total of 33 samples, representing all parts of the late Pleistocene cone, range in SiO_2 content from 55 to 63 weight percent (table 1).

The well-preserved south and east slopes of the cone are radially corrugated by blocky to rubbly levees of numerous overlapping andesitic lava flows. Many such flows bifurcate, most thicken downslope (typically from less than 15 m proximally to 60 m or more on gentler slopes at the foot of the cone), and a few flows grade into distal lobes of disintegrated rubble. Some of the interlevee channels have been deepened into icy couloirs or, lower on the cone, by snowmelt runoff into sharp unglaciated gulches, thus accentuating the radially furrowed aspect of the surface (fig. 2). Only a few such gullies cut deeply enough to expose two or more lava flows.

The north slopes of the outer cone are more eroded, supporting five small present-day glaciers, but the slopes retain their grossly concave constructional form, and parts of the interfluves between the thin ice tongues are near-primary surfaces. In particular, the most easterly of the five glaciers heads 200 m lower than the amphitheater rim and 800 m east of it, in a spoon-shaped cirque that is sharply but shallowly cut into an otherwise-unglaciated surface of steeply leveed andesite flows. Unlike the single narrow glacier that issues from the southwest notch (figs. 4–7), none of the five northerly glaciers is fed from the summit icefield, which remains confined on its north and east sides by the well-preserved amphitheater rim (figs. 5, 7). All five northerly glaciers head in shallow cirques high on the outer slopes of the cone and end on the cone's lower apron in complex accumulations of till, avalanche debris, and reworked 1912 pumice. Even during their maximum advances (2–3 km beyond present termini), all five glaciers terminated on the cone itself, did not coalesce into a unified slope glacier, and left no evidence of ever having joined the broad glacial valleys of Ikagluik and Knife Creeks, which were shaped by the Pleistocene ice that extended many tens of kilometers northwestward (Muller, 1952, 1953; Riehle and Detterman, 1993). We thus infer that all the glaciers now on the cone originated after late Pleistocene recession of major trunk glaciers and that surface lavas armoring the outer cone of Mount Griggs postdate the Last Glacial Maximum (LGM, 25–15 ka).

Four exposures of lava flows that crop out around the base of the cone warrant special discussion because each flow has undergone moderate erosion but appears to underlie with approximate conformity the little-modified surface flows just described. First, at the north toe of the cone, a till-strewn, cliff-forming andesite lava flow (57.9 weight percent SiO_2) that drapes the contact between Jurassic and Tertiary basement rocks is at least 100 m (possibly 150 m) thick; it may have been ponded or otherwise obstructed there, conceivably by ice during the LGM. A fine fresh sample of the lava yielded only 0.3 percent radiogenic Ar and a nominal K-Ar age of 15±18 ka (fig. 4; table 2), thereby supporting our field interpretation that this glaciated flow is young and belongs to the late Pleistocene edifice.

Second, isolated by ice and till at the northeast toe of the volcano, a lightly glaciated andesitic lava flow (57.3 weight percent SiO_2), at least 80 m thick, rests directly on Jurassic basement and dips moderately outboard, consistent with being an early flow from the existing outer cone. Although the flow interior crops out slabby and strongly jointed on cliffs facing the adjacent glacial trough, the flow surface (though scoured) retains blocky remnants that suggest a rather limited history of glacial erosion. The lava gave a whole-rock K-Ar age of 54±8 ka (fig. 4; table 2), in agreement with that inference.

Figure 5. Aerial photograph of summit of Mount Griggs. Amphitheater wall and true summit are visible at right; beheaded lava flows are visible at rim of outer cone. Holocene inner cone topped by nested craters is visible at left. Icefield fills semiannular moat that separates inner cone from outer (amphitheater) wall, and it spills southwestward into steep debris-covered glacier tongue at lower left. Fresh white snow covers right half of icefield; left half (tan) is mantled by fallout from 1912 eruption of Novarupta, through which crevasses in underlying ice are visible. Ikagluik Creek is in lowland background. View northward.

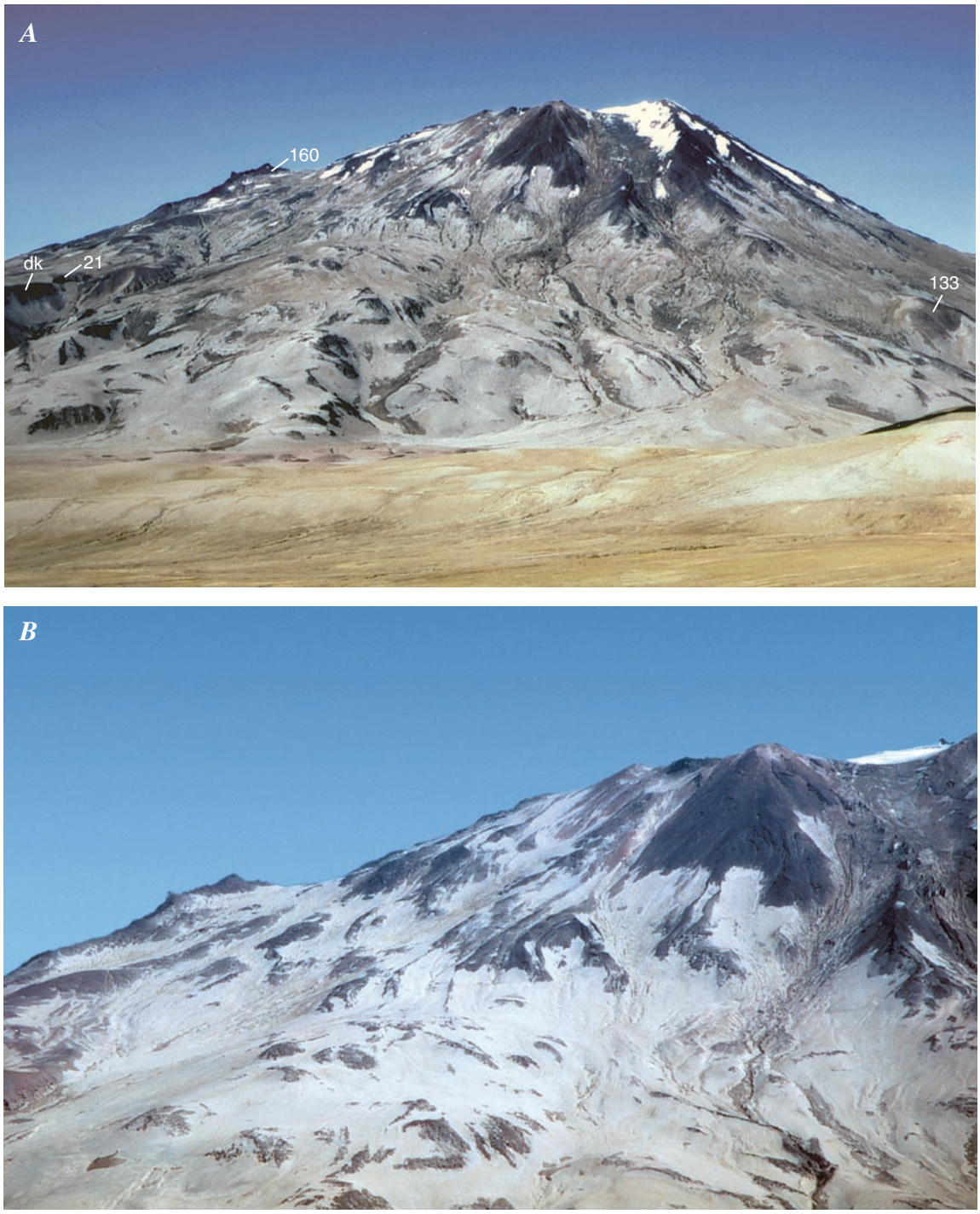

Figure 6. Mount Griggs. *A*, View from floor of the Valley of Ten Thousand Smokes. Near summit, gray-brown debris-covered glacier separates white snowclad east wall of amphitheater in older edifice from black Holocene cone filling it. Foreground slope is Holocene fan of leveed andesitic lava flows, heavily mantled by pumice-fall deposits from 1912 eruption of Novarupta. Toes of lavas are buried by 1912 pyroclastic deposits (oxidized tan where underlain by thick 1912 ignimbrite) and 1-km-wide alluvial fan of 1912 pumice reworked from higher slopes of Mount Griggs. Windows of middle Pleistocene lavas (see fig. 2) crop out at lower right (133 ka) and on left skyline (160 ka). At left edge, Knife Peak debris-avalanche deposit (unit dk) drapes and fills paleorelief cut into stack of andesite lava flows (21±11 ka). View northeastward. *B*, Closeup of upper-central part of figure 6*A*. Debris-covered glacier issues from white snow-covered icefield separating black inner cone from wall of amphitheater at upper right. True summit pinnacle rises behind bergschrund at right rear. Steep black slope of Holocene inner cone consists of andesitic agglutinate, thin spatter-fed lava tongues, and scoriaceous rubble. On left skyline, frost-shattered crags are a window of middle Pleistocene lavas. At center, youngest lava-producing eruption at Mount Griggs issued from top of inner cone and left a steep narrow leveed channel, which (below slope break) spread into a heap of overlapping lava lobes (unit y*, fig. 4), conspicuous in foreground beneath mantle of 1912 pumice.

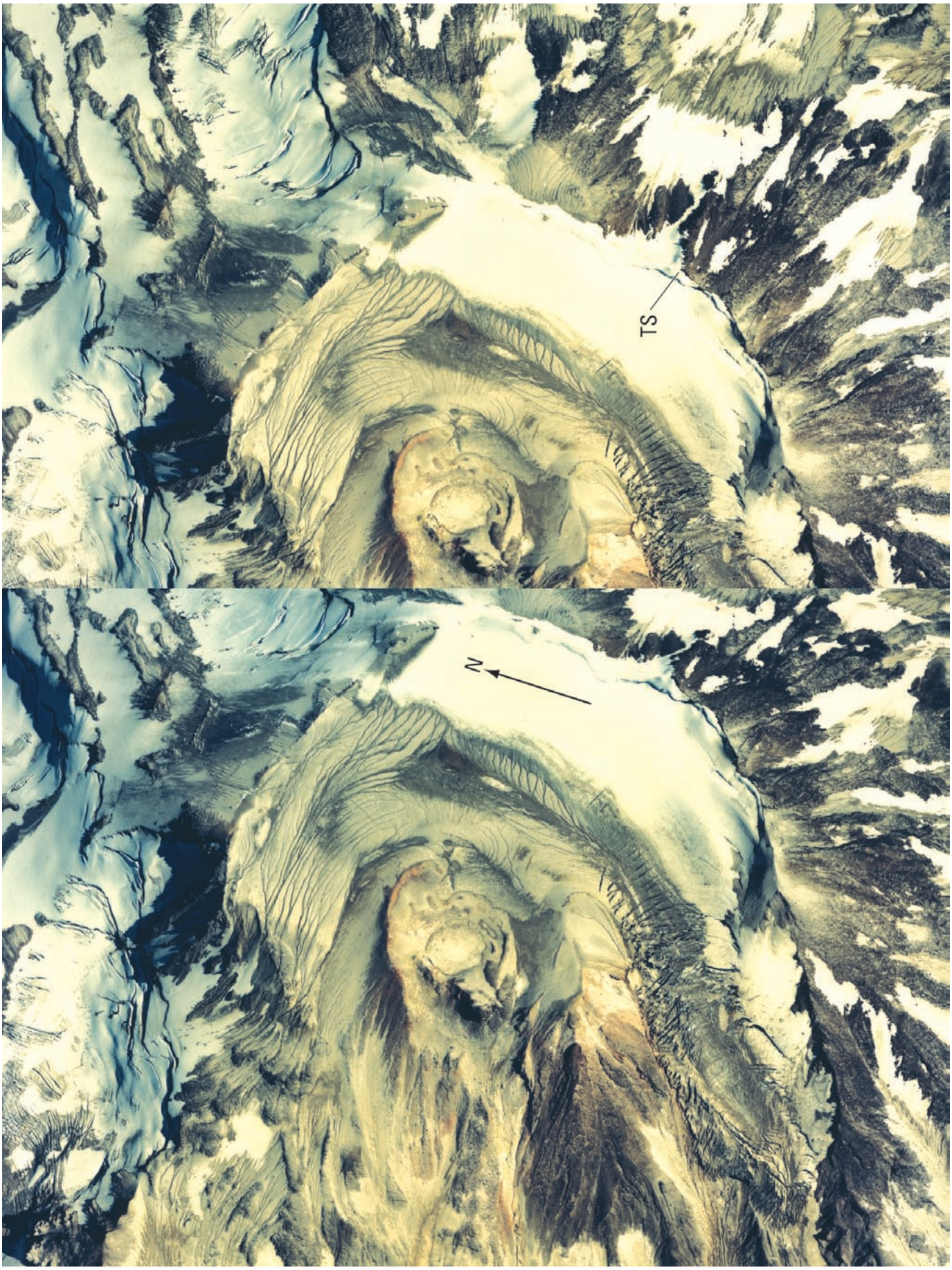
TS
N

Third, at the east base of the volcano, a black glassy lava flow of silicic andesite (62.8 weight percent SiO_2), as much as 200 m thick—the thickest flow recognized at Mount Griggs—directly underlies an uneroded summit-derived andesite flow (60.3 weight percent SiO_2) with apparent conformity. Only the distal 500 m of the thick flow is exposed, owing to the overlap of younger lava flows. Uniquely among Mount Griggs lavas on the east side of the mountain, this thick flow descends to the floor of a deep canyon, here a tributary of Ikagluik Creek (figs. 3, 4). The steep present-day front of the flow has been erosively modified, but its great thickness, its pervasive glassiness, its blocky top, and the extensive columnar joints that dominate its lower half all suggest an intracanyon lava lobe that ponded against a valley-filling glacier. Ice flooring this canyon would presumably have been a branch of a more extensive precursor of present-day Ikagluik Glacier, which is fed by icefields on the north side of Mount Katmai. The thick flow, which yielded a whole-rock K-Ar age of 90±7 ka (table 2), may predate construction of the main late Pleistocene cone or, alternatively, could be the oldest exposed product of that cone.

Fourth, along a gorge on the lower west flank of Mount Griggs, a radial strip of glacially eroded lavas is exposed beneath a major debris-avalanche deposit and an adjacent fan of postglacial lava flows (figs. 2, 4, 6). On the north wall of the 150-m-deep gorge, a northwest-dipping stack of three or more andesitic lava flows (56.3–57.2 weight percent SiO_2) is exposed beneath the avalanche deposit. The platy interior of the top flow gave a whole-rock K-Ar age of 21±11 ka (table 2), consistent with the stack being a component of the late Pleistocene outer cone (rather than a window into a deeply eroded older edifice). Across the gorge and forming much of its south wall is a convolutely flow-foliated dacitic lava flow (63.0–63.4 weight percent SiO_2), pervasively glassy and vesicular and exposed to a thickness of 50 m. The surface of the gray-brown-weathering lava has been moderately scoured, either by ice or by passage of the debris avalanche (part of which overlaps the upper end of the dacite outcrop). Although its contact with the stack of andesites across the gorge is concealed by pumiceous scree, the dacite appears to be inset against them and thus younger. Farther down the gorge, the dacite overlies a locally exposed ledge of andesitic lava (57.6 weight percent SiO_2) similar to those in the stack. Two attempts to date the dacite failed to yield measurable radiogenic Ar, supporting the inference that this lava flow, the most silicic and most potassic recognized at Mount Griggs, was a fairly late product of the late Pleistocene outer cone.

Early Holocene Sector Collapse

The southwest quadrant of the upper part of the late Pleistocene cone slid away into what is now the Valley of Ten Thousand Smokes at some poorly constrained point in early postglacial time—probably early in the Holocene, when the Knife Creek glaciers still occupied the valley as far as Three Forks (fig. 3). The sector collapse left a 1,500-m-wide amphitheater, around which a horseshoe-shaped, 2.5-km-long outer rim is still well preserved (figs. 4, 5, 7). We have recognized no evidence that the failure was accompanied by a magmatic eruption, although neither intrusive triggering of collapse nor eruptive accompaniment would be unusual or unexpected, or, on the other hand, necessary. Weakening of the central core of the upper edifice by (locally focused) acid alteration certainly played a role, because the avalanche deposit is rich in altered debris. The amphitheater depth (and thus the avalanche volume) is unknown because it was later largely filled by the inner andesite cone. How far down the mountain's flank the primary basal slip plane of the detaching slide mass extended is also unknown, because the 12-km^2-area fan of younger lavas wholly covers the scar. Nonetheless, because the area from which the avalanche separated appears to have been no smaller than 3 km^2, the volume excavated is likely to have been no less than 1 km^3. The main remnant of the slide mass, an internally chaotic deposit, locally as much as 200 m thick, mantles a 5-km^2 area of the volcano's lower west slope (fig. 4). Hummocks and other small remnants of avalanche breccia are found as far away as Windy Creek (fig. 3), 10 to 12 km from the base of Mount Griggs, suggesting that the volume excavated could have been as great as 2 km^3. A large fraction of the debris-avalanche sheet must have been emplaced on the floor of Knife Creek valley, where it was reworked as till by Holocene glaciers or concealed by 1912 ignimbrite. An unknown fraction of the avalanche material probably transformed into water-rich debris flows down the valley of the Ukak River. Evidence limiting the age of the sector collapse, and characteristics of the avalanche deposit (here called the Knife Peak debris-avalanche deposit, to distinguish it from younger, similar but smaller examples), are discussed below in the section entitled "Debris-Avalanche Deposits."

◄ **Figure 7.** Stereopair of vertical aerial photographs illustrating summit-crater complex atop Mount Griggs. North arrow (N) and true summit (TS) are labeled on semiannular icefield confined between outer amphitheater rim and inner cone, which has two nested craters and a plug remnant. Crevassed icefield spills leftward into narrow southern glacier. Visible at top are source cirques, steep but shallow, of glaciers on outer slopes of edifice (fig. 4). Coarse stratified ejecta of inner cone stand out on its oxidized north rim and its steep south slope, where light colored owing to fumarolic alteration. Steep black slope southwest of craters consists of leveed andesitic lava flows, many of them thin and spatter fed. On all but steepest slopes, gullied tan deposit of fallout from 1912 eruption of Novarupta obscures surface details, covering all but highest levees of Holocene lava-flow apron to west (left).

Holocene Inner Cone

The amphitheater excavated from the main outer cone by sector collapse has been nearly filled by growth of a new inner andesite cone, which consists predominantly of lava flows, accompanied by subordinate proximal ejecta. A total of 18 samples range in SiO_2 content from 55 to 62 weight percent (table 1). The new cone was fed centrally, with its conduit directly below the previously destroyed summit or, possibly, slightly west of it. The best-exposed part of the inner cone is its black southwest shoulder (fig. 6), which is

steep enough to have been swept free of the mantle of 1912 fallout. Though capped by about 10 m of poorly sorted, unconsolidated, stratified ejecta, the black shoulder itself consists mostly of sheets of varyingly agglutinated scoria and spatter, as well as thin, spatter-fed lava flows (55 weight percent SiO_2), a few of which were substantial enough to feed narrow, kilometer-long leveed tongues of rubbly lava (fig. 6). Wrapping the south slope of the black shoulder is a debris-covered glacier that issues from the summit icefield and follows a gulch which marks the contact between the amphitheater wall of the old cone and the fan of younger lavas from the inner cone (figs. 2, 4–7). The younger cone almost filled the amphitheater but did not quite reach its rim except at the extreme northwest end, where the young lava fan overspilled the rim, buried it, and poured downslope to the cliffs above the northwestern glacier, where some flows broke up over the cirque headwall and others banked against the crags of the 160-ka window.

The lava fan itself covers a 12-km^2 area, extending from the summit craters to the floor of Knife Creek, where some flows continue an unknown distance beneath valley-filling 1912 ignimbrite. On the fan are exposed as many as 20 separate lobes and overlapping leveed tongues of lava, but an unknown (probably far larger) number of flows are buried by those on the surface. Many bifurcate downslope, especially on the gentler lower half of the cone. In particular, the youngest flow (57.2 weight percent SiO_2; unit y*, fig. 4), which emerges near the base of the innermost summit crater, changes at 4,500-ft (1,370 m) elevation from a steep, narrow, leveed channel to a bulging piedmont lobe marked by several subordinate distributary lobes (fig. 6).

Because the gullies between flows are shallow and choked with remobilized 1912 pumice (fig. 6), flow thicknesses are hard to estimate, but some distal lobes are at least 60 m thick. On steeper slopes higher on the cone, they are far thinner. Owing to the pumice scree, flow bases have not been observed, although fused flow-breccia zones (presumed to be near basal) are exposed in a few distal gulches.

Flow surfaces are glassy, vesicular (commonly scoriaceous), and rubbly to blocky; distally, a few are marked by crags and spires, as much as 3 to 4 m high. Though virtually uneroded, flow surfaces apparently show a modest range in degradation of such primary roughness that may reflect a range of ages. The variation in composition likewise suggests that the lava-flow fan represents more than a single eruptive episode. One of the youngest andesite flows crossed over the dacitic lava on the west apron and poured down the gorge cut through the Knife Peak debris-avalanche deposit (fig. 4). Although this rubbly scoriaceous intracanyon lava is readily erodible, the gorge has still not everywhere reestablished a channel completely through it. No soils, accumulations of loess, or tephra layers (all common on nearby surfaces of comparably low relief) have been found atop the young lava fan, although the several meters of 1912 pumice might well conceal some such deposits. Many lavas on the fan surface are probably of late Holocene age, but no evidence is at hand to date them more closely.

Nested Craters and Fumaroles

Inside the 1,500-m-wide amphitheater, the Holocene inner cone is topped by two nested craters (figs. 5, 7), each shallow but steep walled, the outer of which has a maximum (north-south) dimension of 500 m and (like the amphitheater) is also open to the west. The innermost crater is a closed depression, 150 by 200 m wide, slightly elongate north-south, and floored by snow, ice, and the 1912 pumice-fall deposit. These relations and the features described below are best illustrated by the stereopair shown in figure 7.

Where not obscured by 1912 fallout, the rims of both craters are seen to consist of a combination of agglutinate and outboard-dipping lava flows (both effusive and spatter fed) beheaded by the crater walls and draped by poorly sorted blocky ejecta. Stacks of thin overlapping lavas (55 weight percent SiO_2) are best exposed on the black shoulder (fig. 6) that forms the southwest slope of the cone, but a similarly steep outboard slope of thin rubbly flows starts at the northwest rim of the outer crater. The east rim of the innermost crater is pumice mantled, but its west rim is well exposed, consisting of thin, west-dipping andesitic lavas (59–60 weight percent SiO_2) and an 80-m-wide knob of massive andesite (60.4 weight percent SiO_2) that may be a plug remnant.

Locally derived ejecta is best exposed on walls of the outer crater, where coarse, poorly sorted, stratified deposits mantle its rim and make up many of the exposures inside the rim. A rubble-rich coarse-ash matrix encloses angular blocks of dense glassy lava, as large as 1 to 3 m across. Prismatically jointed blocks occur sparsely, and strongly vesicular blocks and scoriae are notably uncommon. Nearly all the ejecta observed appears to have been emplaced by phreatomagmatic or phreatic explosions, probably partly during excavation of the innermost crater. The only scoria-fall deposit observed is on the northwest rim of the amphitheater, where scattered andesitic scoria bombs (55 weight percent SiO_2) armor a wind-deflated surface.

Two clusters of sulfur-depositing fumaroles are active (1) at 7,200- to 7,400-ft (2,195–2,255 m) elevation on the north and west walls of the innermost crater and just downslope outside the west rim, and (2) farther downslope at 6,400- to 6,700-ft (1,950–2,040 m) elevation along a conspicuous gully about 500 m southwest of the rim. The near-rim group releases boiling-point gas from dozens of orifices with weak to moderate discharge; the lower group also has lots of weak fumaroles but includes at least three vigorous jets that emit superheated gas. In July 1979, D.A. Johnston of the U.S. Geological Survey (USGS) measured gas temperatures as high as 108ºC (fig. 8) for the lower group and as high as 99ºC for the upper group. Repeatedly remeasured by R.B. Symonds (oral commun., 1998) from 1994 to 1998, the maximum July temperature of the lower cluster had declined to 99ºC, and of the upper cluster to the boiling point. Several gas samples taken by Johnston and by Symonds consisted of 97 to 99 volume percent steam but also contained significant amounts of CO_2 and H_2S and yielded C- and He-isotopic ratios typical of magmatic gas from arc volcanoes. Relative to fumarolic

gases sampled at Mageik and Trident Volcanoes on the nearby arc front, those from Mount Griggs are notably He enriched, have higher He/Ar ratios, and have elevated $^3He/^4He$ ratios (7.7 times the atmospheric value), probably indicative of a larger proximate contribution from the mantle (Poreda and Craig, 1989; Sheppard and others, 1992).

Composition of Eruptive Products

Most lava flows exposed on Mount Griggs and a few near-vent scoria bombs were sampled, as were lava blocks from several debris-avalanche deposits. Some 77 samples were analyzed by X-ray-fluorescence spectroscopy (fig. 9; table 1). Nearly all samples are mafic to silicic andesite (54.9–63.4 weight percent SiO_2), and only a single lava flow (63.0–63.4 weight percent SiO_2), low on the west flank, is formally a dacite. In addition, a single mafic lava (probably olivine accumulative) and two mafic magmatic enclaves contain 50.9, 53.6, and 53.9 weight percent SiO_2, respectively. The range in SiO_2 content for the eruptive suite at Mount Griggs is similar (not identical) to those of nearby Alagogshak, Martin, Mageik, Trident, and Snowy Mountain volcanoes but is far more restricted than those of Mount Katmai and Novarupta (Hildreth and Fierstein, 2000).

All rocks collected are plagioclase-rich two-pyroxene andesites, with subordinate olivine and Fe-Ti oxides in every sample. Though seldom abundant, olivine is virtually ubiquitous in the eruptive products of Mount Griggs and is certainly more common than at any of the neighboring volcanoes. Remarkably, not a single Mount Griggs sample fails to be phenocryst rich; virtually all samples contain 25 to 60 volume percent crystals larger than 0.1 mm across. Kosco (1981) point-counted thin sections of 13 Mount Griggs lavas, obtaining a range of 31–58 volume percent phenocrysts. Nearly all samples have a glassy or partly glassy groundmass, and (where exposed by erosion) even the platy interior zones of many lava flows retain a little glass. Polycrystalline clots of the main phenocryst phases (in varied combinations and proportions) are common, as are microdioritic clots and still-finer-grained mafic blebs. As in many andesites, plagioclase crystals of several generations, reflecting mixed origins and contrasting histories of dissolution and growth (Singer and others, 1995; Coombs and others, 2000), are present in most samples. Magmatic enclaves, typically 1 to 15 cm across and generally finer grained and more mafic than the host andesite, occur in many Mount Griggs lavas, but they are much less abundant than at nearby Trident Volcano.

Fully opacitized ovoids and prisms sparsely present in a few samples may once have been amphiboles, but no relict amphibole has been positively identified. Although no biotite has been observed, apatite needles are included within plagioclase phenocrysts in most or all samples. Kosco (1981) reported traces of quartz in two olivine-bearing andesite samples (57 and 59 weight percent SiO_2) from Mount Griggs, and, consistent with xenocrystic disequilibrium, he mentioned reaction rims around them. Kosco also reported traces of sanidine in two samples (60 weight percent SiO_2), and because the sanidine is untwinned and unzoned (Or_{65}), it might be cognate, possibly reflecting the advanced crystallinity of the phenocryst-rich magmas. Microprobe determinations by Kosco for the major phenocryst phases in several Mount Griggs samples (for which he did not provide locations) yielded the following: (1) olivine is $Fo_{64–82}$ and has limited normal zoning in individual crystals, (2) pyroxenes have only slight (normal or reversed) zoning and are confined to the augite and hypersthene compositional ranges, and (3) complexly zoned plagioclase has compositional ranges of $An_{55–82}$ in clear phenocrysts and $An_{52–87}$ in sieved crystals replete with glass inclusions.

Figure 8. David A. Johnston sampling gas emitted vigorously at one of several sulfur-precipitating fumaroles along a gulch about 400 m southwest and downslope from rim of innermost crater of Mount Griggs (where additional fumaroles also occur). The Juhle Fork of Knife Creek and the Valley of Ten Thousand Smokes are in left background. Hottest fumarole measured was 108ºC in 1979. Photograph by Peter Shearer, then of the U.S. Geological Survey, taken July 2, 1979. Some 321 days later, Johnston was swept away (in all but memory) by the May 18, 1980, eruption of Mount St. Helens.

Whole-rock data for all 77 samples from Mount Griggs (table 1) plot as a narrow array virtually central to the medium-K field of figure 9*A*. The K_2O-SiO_2 panel further illustrates that the eruptive products of Mount Griggs are consistently K enriched relative to the neighboring volcanoes, providing a ready discriminant for samples of uncertain provenance. Nearly all Mount Griggs samples fall in the calc-alkaline field on the conventional tholeiitic-versus-calc-alkaline discrimination diagram (FeO*/MgO ratio versus SiO_2 content; not shown) of Miyashiro (1974). The alkali-lime intersection falls at 61 to 62 weight percent SiO_2 (fig. 9*B*), also defining a calc-alkaline suite, according to the original scheme of Peacock (1931). In this respect, Mount Griggs contrasts with the nearby volcanic-front centers, which all have calcic intersections at 63 to 64 weight percent SiO_2 (Hildreth, 1983; Hildreth and others, 1999, 2000, 2001).

The eruptive products of Mount Griggs represent a typical low-Ti arc suite, containing only 0.63 to 0.90 weight percent

TiO_2. None of the samples is notably primitive, because MgO content ranges from only 1.6 to 5.1 weight percent for the main array, and the three mafic mavericks are only slightly more magnesian. Kosco (1981) provided X-ray-fluorescence data that included 10 to 14 ppm Ni for 7 Mount Griggs samples and 16 to 60 ppm Cu and 60 to 75 ppm Zn for 25 Mount Griggs samples.

Al_2O_3 and P_2O_5 contents are ordinary for arc suites, ranging from 16.5 to 19.3 weight percent and from 0.14 to 0.28 weight percent, respectively, although both components are somewhat elevated relative to products of the neighboring centers. Sr contents (table 1) are scattered, ranging from 315 to 432 ppm, but tend (along with many Trident lavas) to be elevated relative to other volcanoes in the Katmai cluster (Hildreth and Fierstein, 2000). Rb contents range from 18 to 43 ppm (with the three mafic mavericks at 10–13 ppm). On a plot of Rb versus SiO_2 content (not shown), the Mount Griggs suite is elevated in Rb relative to the volcanic-front arrays, but it partly overlaps them rather than providing the nearly clean discrimination shown by the K_2O-SiO_2 panel (fig. 9*A*). Similarly but conversely, most Mount Griggs lavas are slightly Fe poorer than products of the neighboring volcanoes, although the arrays again show partial overlap (see Hildreth and Fierstein, 2000, fig. 10).

Like the K_2O-SiO_2 panel, a plot of Zr versus SiO_2 content (fig. 9*C*) provides a first-order distinction between arrays for neighboring volcanoes on the main volcanic line and the Mount Griggs suite, which has relatively elevated Zr contents of 106 to 205 ppm (with the three mafic mavericks having 78, 94, and 109 ppm). Moreover, the Zr-SiO_2 plot is the only variation diagram that suggests any systematic compositional change over time among the eruptive products of Mount Griggs. Figure 9*C* shows that most (but not all) samples from the middle Pleistocene windows are Zr deficient relative to the main late Pleistocene and Holocene data array.

In summary, the andesitic suite at Mount Griggs resembles those of the contemporaneous centers on the nearby volcanic front but contains more olivine, has marginally lower Fe contents, tends to be relatively enriched in Al, P, Rb, and Sr, and is consistently more enriched in K and Zr. Moreover, the Mount Griggs array lacks silicic members.

Geochronology

We measured K-Ar ages on whole-rock samples from each of the three glaciated windows of older lavas and from five distal exposures around the base of the late Pleistocene cone (fig. 4; table 2). Sample-selection criteria and analytical methods were described by Hildreth and Lanphere (1994). Seeking high-precision ages for late Pleistocene rocks, we used the multiple-collector mass spectrometer (Stacey and others, 1981) at the USGS laboratories in Menlo Park, Calif.

The north, west, and south windows yield K-Ar ages of 292±11, 160±8, and 133±25 ka, respectively (table 2). Such widely spaced ages for glaciated remnants exposed, respectively, 1,600, 500, and 1,300 m lower than the modern summit signify that much of a long-lived middle Pleistocene edifice had been eroded away before being extensively covered by the late Pleistocene cone.

The stratigraphically lowest lava that appears to have been erupted from the late Pleistocene cone flowed eastward to the floor of a glacial canyon tributary to Ikagluik Creek; it yielded an age of 90±7 ka. A second thick basal lava flow resting on Jurassic basement rocks at the northeast toe of the cone gave an age of 54±8 ka. If these lavas indeed issued from the central vent of the main late Pleistocene cone (rather than from a wrecked predecessor edifice), their antiquity implies exposure to erosion for several tens of thousands of years for interim slopes of the cone that are now concealed by the carapace of little-modified lava flows that evidently postdate the LGM.

We attempted to date three additional lava flows from other parts of the late Pleistocene cone. To the north, a thick distal andesite flow that overlies the contact between Jurassic and Tertiary basement rocks (fig. 4) gave an age of 15±18 ka. On the west slope, the top andesite flow underlying the Knife Peak debris-avalanche deposit gave an age of 21±11 ka. Adjacent to the top andesite flow, the lone dacitic lava flow exposed at Mount Griggs failed to yield measurable radiogenic Ar despite repeated extractions. Erosion and scour of the dacite may not have been glacial, as we had first assumed, but may instead reflect passage of the debris avalanche and subsequent Holocene incision of the adjacent gorge.

Radiocarbon ages for Holocene surficial deposits that limit the emplacement ages of debris avalanches at Mount Griggs are discussed below in the section entitled "Debris-Avalanche Deposits."

Eruptive Volumes

Mount Griggs has undergone glacial erosion throughout its existence; the modern climate being globally one of the mildest during its 300-k.y. lifetime. During glacial maximums, ice sheets blanketed the regional topography to above 4,000-ft (1,220 m) elevations (Riehle and Detterman, 1993; Mann and Peteet, 1994), locally extended higher against horns and nunataks, and repeatedly ravaged the edifice of Mount Griggs. Partly for this reason, the pre-late Pleistocene eruptive volume cannot be estimated with any accuracy.

Mount Griggs today covers an area of about 60 km^2. The amphitheater rim is now as high as 2,330 m, and so the precollapse summit certainly reached at least 2,350 m. On the apron, lavas extend as low as 1,800 ft (550 m) elevation on the north and southwest and down to 2,800- to 3,000-ft (855–915 m) elevation in other sectors. Basement rocks, however, crop out at as high as 4,400-ft (1,340 m) elevation on the east and west flanks of the cone and at 3,100- to 3,500-ft (945–1,070 m) elevation along the north toe but are not exposed along the south toe of the cone where it meets the valley floor at 1,800- to 2,300-ft (550–700 m) elevation. Using these data, various sectorial cone-model approximations yield volumes in the range 23–30 km^3; the main uncertainty is in the basement topography buried by the edifice. Taking in account the concavity of the cone's

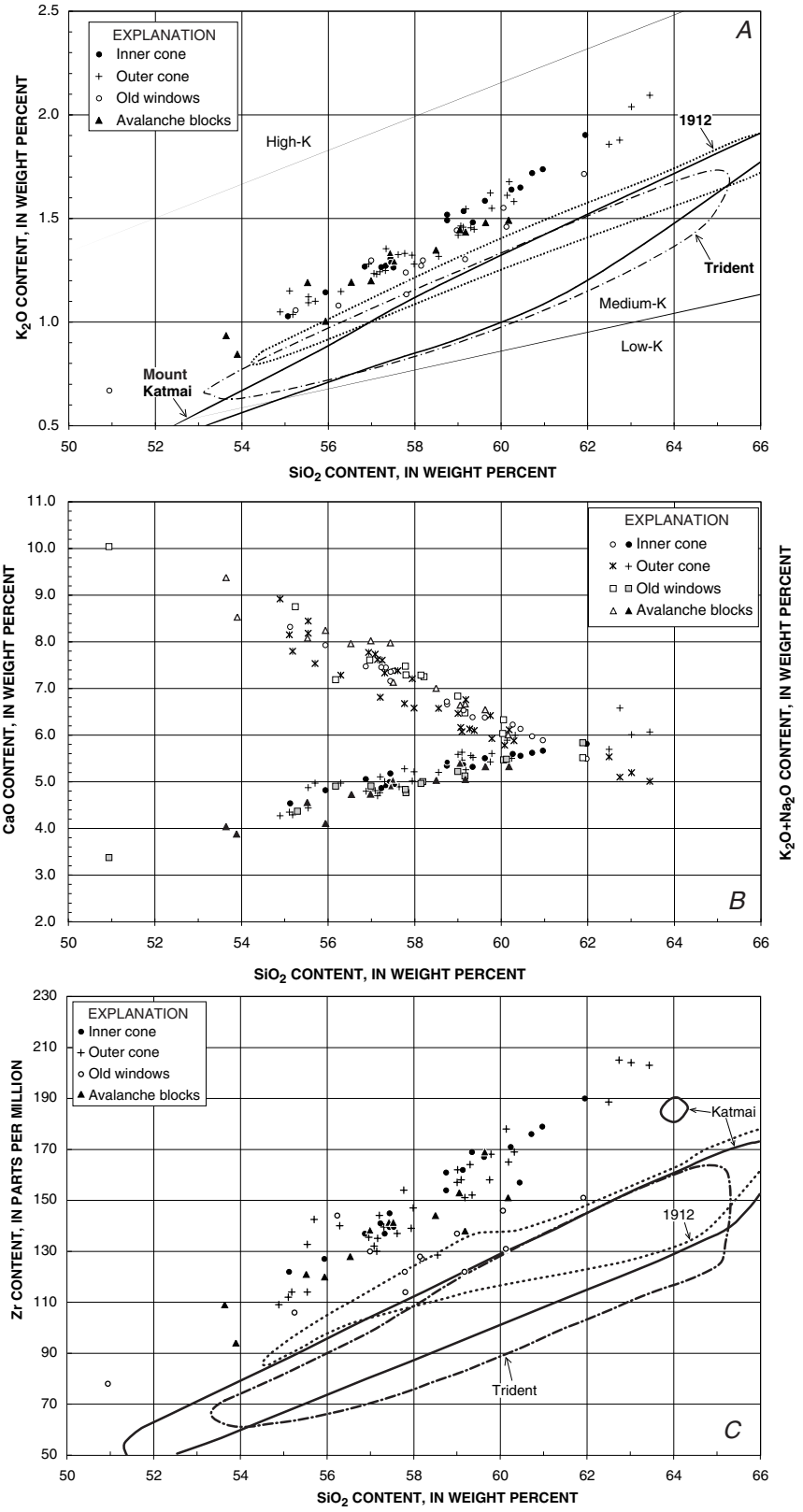

Figure 9. Whole-rock compositional data for 77 samples from Mount Griggs (table 1), as identified in inset. *A*, K_2O versus SiO_2 contents. *B*, CaO (upper trend) and total alkalies (lower trend) versus SiO_2 contents. *C*, Zr versus SiO_2 contents. Enclosed fields in figures 9*A* and 9*C* show comparative arrays from neighboring volcanoes, Mount Katmai and Trident, and from zoned suite from 1912 eruption of Novarupta (Hildreth and Fierstein, 2000). Mount Katmai and 1912 arrays extend off panel to rhyolitic compositions, whereas those of Mount Griggs and Trident are limited to andesite-dacite range.

slopes, a conservative estimate places the present-day total volume of the volcano in the range 20–25 km^3.

Eruptive volumes of older eroded components of the edifice are even harder to reconstruct with acceptable accuracy. The southern and northern windows are basal-distal, and the craggy western window exposes a stack of lava flows at 6,200-ft (1,890 m) elevation that dips 20–25° W., away from a former summit that may well have been as high or higher than today's. If the middle Pleistocene edifice had indeed been as large as the present one, then the distribution of old windows suggests that at least half of it had been removed before construction of the late Pleistocene cone, implying an erosive loss of at least 10 km^3 and thus a total eruptive volume in the range 30–35 km^3. Such an estimate is surely conservative because (1) off-edifice fallout (probably limited) and intracanyon lavas and mass flows (possibly substantial) later wholly removed by erosion are not taken into account; and, perhaps more important, (2) the argument condenses Pleistocene glacial erosion into a continuous process that resulted in a net loss of 10 km^3, although we know that the edifice underwent episodes of constructive growth at about 292, 160, 133, and 90 ka. How many times it was partly torn down is unknown.

For a 300-k.y. lifetime, an eruptive volume of 35 km^3 implies an average productivity of 0.12 km^3/k.y. Such long-term averaging surely obscures sporadic episodes of far greater productivity. If most of the late Pleistocene cone was constructed between 54 and 10 ka, our estimates yield 15 $km^3 \div 44$ k.y.=0.34 km^3/k.y. for an interval that probably itself consisted of several cone-growth episodes. Finally, for the inner cone and southwest lava fan, the Holocene eruption rate is estimated at 2.2 $km^3 \div 10$ k.y.=0.22 km^3/k.y. These productivities are in the normal range for well-studied stratovolcanoes but far below those of major episodes (≥5 km^3/k.y.; Hildreth and Lanphere, 1994). Locally, the long-term eruption rate for Mount Griggs is similar to that of the Trident cluster, greater than that of Snowy Mountain, and lower than those of Mounts Katmai and Mageik, both of which have produced volumes similar to or larger than that of Mount Griggs in a third the time (Hildreth and Fierstein, 2000; Hildreth and others, 2000, 2001).

Debris-Avalanche Deposits

Five poorly sorted, chaotic deposits dominated by andesite blocks have been recognized on the lower slopes of Mount Griggs, one of late Pleistocene age and the others of early Holocene age. All of these deposits appear to have resulted from avalanches that broke loose high on the volcano. We discuss them below in apparent order of emplacement.

Diamict of Griggs Fork

A coarse diamict, as thick as 70 m, is exposed for about 2 km along a scarp bounding the valley floor at the south foot of the volcano (unit ds, fig. 4). West of the Griggs Fork of Knife Creek, it underlies an area of at least 1.2 km^2, probably as much as 2 km^2. The unstratified deposit is overlain variously by till, andesitic lava flows of the late Pleistocene cone, indurated remnants of a scoria-flow deposit from Mount Katmai, and 1912 ignimbrite and fallout. Though widely obscured by these deposits, the diamict is exposed (fig. 10) along two deep gorges (figs. 2, 4) that interrupt the scarp at the south toe of Mount Griggs. A lag of andesite blocks typically armors deflated surfaces and sideslopes (fig. 10). The diamict may rest on Jurassic basement at the Griggs Fork (fig. 3), but in the gorges and elsewhere it rests on till (fig. 4), which is distinguishable by its varied clast assemblage.

Stones in the till deposits here are predominantly Jurassic sandstone and siltstone of the Naknek Formation, along with subordinate andesites and porphyritic Tertiary intrusive rocks. In contrast, coarse clasts in the diamict are almost exclusively massive to scoriaceous andesite, mostly angular to subangular, abundantly 0.2 to 2 m across, some as large as 3 m across. Many of the dense angular blocks retain reddened joint surfaces that were oxidized during posteruptive cooling, and both black and oxidized scoria is common among clasts smaller than 10 cm across. Most blocks are fresh andesite, dark gray or brick red, and a few have alteration rinds 1 to 2 cm thick. Hydrothermally altered andesite clasts, ochre to cream yellow, are present but not abundant, and few are larger than 10 cm across. Unlike many debris-avalanche deposits (including the others at Mount Griggs), no large (10- to 100-m scale), quasi-coherent, incompletely disaggregated domains are observed, and big composite blocks are sparse. Rounding of dense clasts is virtually absent, as are the streamlined shapes and striae that mark some clasts in the subjacent till.

The matrix is poorly sorted, fines-poor, dark-gray-brown, dominantly sand- to gravel-grade andesitic debris, evidently partly derived by breakage of the enclosed blocks. The deposit is barren of vegetation, in contrast to the underlying till, which supports scattered patches of mosses, grasses, and dwarf willows (fig. 10*A*), probably owing to the greater silt and clay fraction in the till matrix.

The characteristics of the deposit suggest that it was not the product of a sector collapse and that its source area was not an extensively altered part of the edifice. The diamict is not a glacial deposit, as shown by the absence of fines, the absence of the main basement-rock types exposed nearby, and its contrasts with the directly subjacent till. The deposit appears not to have resulted from breakup of a lava flow actively extruding high on the edifice because the deposit is unstratified, very thick (25–70 m), and shows little or no evidence of hot emplacement. Our tentative conclusion is that a stack of lava flows on a relatively unaltered part of the edifice failed abruptly, avalanched down the steep rubbly dipslope of the stratocone, broke up extensively during transit, and was emplaced as a single chaotic sheet, possibly impounded thickly against a valley-filling glacier. Much of the deposit has subsequently been removed by the Knife Creek Glaciers.

No evidence for a source scar remains high on the edifice because construction of the leveed lava-flow surface of the late Pleistocene cone postdates the avalanche and several of

Figure 10. All-andesite diamict west of the lower Griggs Fork of Knife Creek (unit ds; fig. 4). *A*, Eastern of a pair of deep gorges that cut diamict at south foot of Mount Griggs. Black dacitic scoria-flow deposit from Mount Katmai, vaguely stratified, sintered, and 2 to 10 m thick, rests directly on deposit, which is here about 30 m thick. Many blocks on sideslope are 1 to 3 m across. Willow patch at lower left marks top of underlying heterolithologic till, which is fines richer and consists predominantly of nonandesitic basement-rock types. Western gorge (rim in right background) has same stratigraphic sequence. Plateau surfaces are mantled by pale-gray to pinkish-tan fallout and ignimbrite from 1912 eruption of Novarupta, which supply mud dribbling down gorge wall. View northwestward. *B*, Closeup of same diamict shown in figure 10*A* , where exposed on northwest wall of western gorge. Two packs in central foreground provide scale. Angular to subangular andesite clasts, commonly 20 to 150 cm across, form surface-armoring lag that is concentrated by wind deflation of deposit's dark-gray-brown fines-poor matrix, which consists of andesitic sand-and-gravel-grade debris. Pale-gray surface material is 1912 pumice. Gorge floor is at left. The Knife Creek arm of the Valley of Ten Thousand Smokes is visible in distance.

its little-modified surface lavas overlap the deposit. Further evidence of a late Pleistocene age is provided by a sintered black dacitic scoria-flow deposit (itself glacially scoured) that was erupted at Mount Katmai near the end of the Pleistocene and banked against the base of Mount Griggs, directly atop the diamict (fig. 10). Although we have been unable to date the avalanche material directly, its preservation along the valley margin, along with the overlying scoria flow and leveed lava flows, suggests emplacement during waning millennia of the Pleistocene, since the LGM.

Diamict of Ikagluik Creek

At 2,300-m elevation on the rim of a sheer-walled canyon tributary to Ikagluik Creek, a rusty-orange to cream-yellow diamict (unit de, fig. 4) rests directly on Jurassic basement rocks at the brink of the cliff. The deposit is 4 to 12 m thick, crops out along the cliff for 400 m, and contains many 1-m blocks of dark-gray andesite (some with alteration rinds), as well as an abundance of orange, yellow, and white pervasively altered clasts (generally smaller than 20 cm across), in a pale-orange, clay-bearing, silty-sandy matrix. Along with 12 m of overlying gray till, which lacks the altered clasts, the deposit forms a steep unstable slope at the rim of a 200-m-high cliff. Because the outcrop is only 1 km downslope from the present-day snout of the northeastern glacier, the till is likely to be of Neoglacial age, an interpretation strengthened by the thinness of "soil" atop the till. Here, the combined thickness of eolian silt and organic-rich soil is only 10 to 15 cm, whereas on many nearby surfaces the postglacial accumulation is in the range 50–100 cm. The diamict rests on a bedrock surface that may have been scoured clean during the LGM, and if so, its age would be latest Pleistocene or early Holocene. The deposit was evidently emplaced as a modest avalanche that probably originated on the headwall of the northeastern glacier, where its source included hydrothermally altered andesite.

Knife Peak Debris-Avalanche Deposit

By far the most voluminous diamict that originated on Mount Griggs is the avalanche deposit (unit dk, fig. 4) resulting from sector collapse of the late Pleistocene cone. The 1,500-m-wide amphitheater left by catastrophic removal of 1 to 2 km^3 of the edifice was discussed above in the subsection entitled "Early Holocene Sector Collapse," as was extensive healing of the scar by growth of the inner cone and its southwesterly fan of Holocene lava flows.

The 5-km^2-area remnant that forms the lower west slope of the volcano (figs. 2–4) is essentially an "overbank" facies of the avalanche deposit, downslope from the amphitheater and adjacent to the main sector excavated and subsequently refilled by younger lavas. It crops out as high as 5,700-ft (1,740 m) elevation, where it is overlapped by the younger lavas, but its upper expanse is relatively thin (10–30 m thick). At 3,500-ft (1,070 m) elevation, it thickens abruptly to as much as 200 m, apparently filling steep paleotopography where it drapes a stack of lava flows, the uppermost of which yields an age of 21±11 ka. Here, too, the deposit's surface is marked by a 30-m-high radial ridge. The surface of the deposit downslope (fig. 11) is gray brown, undulating but not hummocky, subdued but not glaciated, and slopes an average of 14º to the floor of the Valley of Ten Thousand Smokes. Its toe is truncated by a small scarp, probably a former cutbank adjacent to the alluvial plain of Knife Creek, that is now largely buried by 1912 ignimbrite and fallout.

Figure 11. Pale-pinkish-orange debris-avalanche deposit (unit dj, fig. 4), valley confined along the Juhle Fork of Knife Creek. Irregular brown slope on near side of the Juhle Fork is older, larger Knife Peak debris-avalanche deposit (unit dk), through which the Juhle Fork valley had been cut. In background is lower part of the Valley of Ten Thousand Smokes (VTTS), filled by ignimbrite from 1912 eruption of Novarupta and flanked by brown ridges of subhorizontally stratified Jurassic sedimentary rocks. Salient of pale ignimbrite in top center is Windy Creek embayment of VTTS, where numerous hummocks of larger debris avalanche (figs. 3, 12) are preserved, 10 to 12 km from foot of Mount Griggs. Crossvalley Neoglacial moraine (fig. 3) is discernible in right distance as dark irregular ridge surrounded by pale ignimbrite. View westward.

Mostly chaotic internally, the deposit nonetheless includes quasi-coherent domains, as much as 200 m long, of disrupted but fresh andesitic lavas. Nearby domains, as large as 40 m across, are yellowish orange and rich in shattered blocks of hydrothermally altered andesite. Most exposures look thoroughly scrambled, consisting of lithologically varied andesite clasts in a varicolored matrix that can be pale red, orange brown, yellow, or gray. The matrix is poorly sorted, fines bearing but not fines rich, and predominantly sandy or gravelly. Blocks are commonly 1 to 3 m, and nearly all the larger ones are angular fresh andesite. Some large blocks consist of hydrothermally altered andesite, but most clasts of such weakened material are subrounded and small, typically smaller than 10 cm across. Among fragments smaller than 5 cm across, the proportion of altered clasts may equal or exceed that of fresh ones. Although the blocks are largely fresh material, much, possibly half, of the deposit came from altered parts of the former edifice.

There is good evidence that the 5-km^2-area remnant preserved on the west slope of the edifice is only a modest

fraction of the original avalanche deposit. Windows through 1912 ignimbrite expose accumulations of angular blocks of the andesite of Mount Griggs (as verified chemically; fig. 9; table 1) across Knife Creek on the north noses of Broken and Baked Mountains (figs. 3, 4). Remnants of similar material occur as hillocks and lenses in the Windy Creek embayment of the Valley of Ten Thousand Smokes (fig. 3). On both sides of Windy Creek, conical hummocks, as much as 18 m high, consist of angular fragments of the andesite of Mount Griggs that represent shattered megablocks which crumbled in place (fig. 12).

Some andesite hummocks appear to rest directly on sheets of till, and others rise from stream terraces cut on such till. The till everywhere includes abundant basement clasts (Jurassic sedimentary rocks and Tertiary porphyry), and few or none of the andesitic stones in the till are conspicuously olivine-bearing like the Mount Griggs andesites that make up the hummocks. Some of this till is likely to have been deposited during waning phases of the latest Pleistocene glacial recession, but the local situation here is ambiguous. The receding ice front may not have withdrawn upvalley from Three Forks (fig. 3) until well into the conventional Holocene (that is, later than 10 ka). Moreover, a composite Neoglacial moraine was constructed across the Valley of Ten Thousand Smokes near Three Forks (fig. 3) until as recently as 8–7 ka, either by still-receding ice or by Holocene readvances, although such ice need not (in either scenario) have fully reoccupied the Windy Creek embayment. Inferring the age of the hummocks from their local relations with till thus requires caution and site-specific radiocarbon ages because lithologically similar till of at least three ages is present locally.

Our constraints and reasoning concerning the emplacement age of the Knife Peak debris-avalanche deposit and its distal hummocks are as follows. On the slopes of Mount Griggs, no direct age evidence has been obtained for the main 5-km^2-area remnant, but the younger Juhle Fork debris-avalanche deposit (unit dj, fig. 4; see below) overlies its northwestern margin. As discussed below, the Juhle Fork deposit is itself older than 6,720±140 ^{14}C yr, and so the larger underlying deposit must be still older. We infer that a valley glacier still occupied part of the Knife Creek valley when the sector collapse took place because (1) valley-floor remnants survive only at sites topographically shielded from erosion by such ice; and (2) hummocks and sheets of avalanche debris are absent axially in the Knife Creek valley, both at the crossvalley Holocene moraine near Three Forks (fig. 3) and in exposures (of till) beneath 1912 ignimbrite along the lower gorges of Knife Creek. Moreover, the absence of a continuous avalanche sheet (even in the Windy Creek embayment) suggests that much of the deposit could have been emplaced supraglacially and subsequently removed by glacial transport and by meltwater from the wasting ice. The hummocks (fig. 12) and a few lenses of angular avalanche blocks, all of which overlie till along Windy Creek, would by this reasoning largely represent megablocks that were shunted to the margin of a valley-floor glacier. Transport of andesite megablocks 12 km downvalley to produce the Windy Creek hummocks (now 6–18 m high) is consistent with mobility enhanced by sliding over ice, but the 1,500-m drop in elevation would have provided adequate momentum for such a runout, even without the roughness-reducing contribution of an icy substrate. Until we recognized their all-andesite constitution and Mount Griggs provenance, we had assumed that the Windy Creek hummocks were glacial kames. For those megablocks that may have been emplaced atop wasting ice, rather than marginal to it, the kame-versus-hummock distinction blurs.

Figure 12. One of many conical hummocks preserved along both sides of lower Windy Creek (see fig. 3). Hummocks are 8 to 18 m high, overlie till or alluvial terraces cut on till, and contain angular to subangular blocks of andesite of Mount Griggs (as large as 3 m across) in a dark-gray, poorly sorted matrix of andesitic sand and rubble. All blocks analyzed have distinctive compositions enriched in K and Zr, locally diagnostic of Mount Griggs lavas. All subjacent and nearby glacial deposits are rich in basement clasts that are absent or rare in hummocks.

In summary, because neither the postcollapse lavas, nor many of the youngest precollapse lavas, nor the hummocks, nor the surface of the main 5-km^2-area remnant of the avalanche deposit have been glacially overrun, the sector collapse clearly took place after major withdrawal of the regionally extensive, kilometer-thick ice sheets of the LGM (Riehle and Detterman, 1993; Mann and Peteet, 1994). During the latest Pleistocene and early Holocene, however, a thin valley-floor glacier nonetheless continuously or recurrently occupied the Knife Creek valley, at least as far downvalley as Three Forks and possibly until as recently as 8–7 ka. When the avalanche occurred, ice had partly withdrawn from the Windy Creek embayment but not from the Three Forks area. The sector-collapse event thus predated 8 ka, an inference sustained by a minimum age of 6,720±140 ^{14}C yr B.P. for the Juhle Fork debris-avalanche deposit (see next section), which overlies (and occupies a valley cut into) the Knife Creek debris-avalanche deposit (figs. 4, 11). Four regionally distributed Holocene tephra layers are preserved atop one of the Windy Creek hummocks. Because none of the tephras is older than 6 ka and less than 5 cm of sandy "soil" separates the lowest tephra layer from the top of the hummocky debris, emplacement of the avalanche is unlikely to have been much earlier than 8–7 ka, and so it probably occurred during the early Holocene.

Juhle Fork Debris-Avalanche Deposit

Also during the early Holocene, another small but substantial debris avalanche broke loose from the headwall of the northwestern glacier of Mount Griggs and filled the canyon of the Juhle Fork of Knife Creek, a gorge that had not long previously been cut into the much larger Knife Peak debris-avalanche deposit. As much as 50 m thick at its narrowest point (at 3,000–3,400 ft [915–1,035 m] elevation), the intracanyon Juhle Fork debris-avalanche deposit (unit dj, fig. 4) crops out today over a 2.8-km^2 area, but originally it must have been much more extensive because it remains 30 m thick distally where it adjoins 1912 ignimbrite on the floor of the Valley of Ten Thousand Smokes (fig. 11).

Hummocks are few and subdued on the relatively planar sloping surface of what appears to have been a highly shattered, relatively fluidly flowing avalanche mass. The largest is a 10-m-high conical hummock (fig. 13) at the narrows where the westward proximal flowpath changes abruptly into the southwest-flowing canyon of the Juhle Fork (fig. 4). Relatively few blocks in the deposit are larger than 4 m across, although near the same narrows we did observe an 8-m block of shattered fresh andesite and a 7-m block of yellow to ocher acid-altered andesite, likewise shattered internally. Near the lower end of the deposit, most blocks are smaller than 1 m across, but shattered 2- to 5-m blocks are still present, with many of the acid-altered ones disintegrating into pale-gray, white, or yellow piles of rubble laced with rusty-orange-brown fracture fillings. Virtually all clasts are of andesite, fresh or altered. The matrix is poorly sorted, fines bearing, but mostly sandy to rubbly. Locally, the matrix has brick-red, yellowish-ocher, and gray-brown domains, but in broad view most of the deposit is pale orange, especially along its intracanyon reach, in contrast to its dominantly gray-brown older neighbor (fig. 11). The orange color reflects the alteration zone at the avalanche source, which is now largely ice covered but still partly exposed along the upper north wall of the northwestern glacier (red-stippled zone, fig. 4).

Atop the distal part of the avalanche deposit (and beneath fallout from the 1912 eruption of Novarupta), five thin tephra layers are intercalated within an accumulation of eolian silt and soil, 1.3 m thick. Organic-rich silt just beneath the lowest tephra layer (and separated from the top of the avalanche deposit by approx 20 cm of silt) yielded a radiocarbon age of 6,720±140 ^{14}C yr B.P. (Geochron Gx-23625). The second tephra layer is widespread regionally and known from many sections to have fallen about 6 ka. If the 20 cm of eolian silt below the dated horizon accumulated at the same rate as the 74 cm of silt within the section above it (74 cm÷6.72 k.y.=11 cm/k.y.), then the avalanche deposit could be about 1,800 years older, or about 8,500 years old. Despite the uncertainties, it was clearly emplaced during the early Holocene.

Figure 13. Conical hummock standing 10 m above surface of Juhle Fork debris-avalanche deposit, where its steeper westward proximal path funneled into narrower southwest-trending valley of the Juhle Fork (fig. 4). Note abundance of brown matrix, richer in fines than block-rich deposit shown in figure 12. Andesite clasts visible here are as large as 1.5 m across, but other intact (though internally shattered) blocks nearby are as large as 8 m across. Pale-gray surface veneer is fallout from 1912 eruption of Novarupta. West slope of Mount Griggs is at left in middle distance. View southwestward toward Mount Mageik (left skyline) and the River Lethe arm of the Valley of Ten Thousand Smokes (distant right).

Along the lower 2 km of the Juhle Fork canyon, the avalanche overtopped its left-bank (southeast) wall, first covering a Neoglacial left-lateral moraine and then, near the canyon mouth, spilling out over the Knife Peak debris-avalanche deposit. The moraine consists of gray-brown andesitic debris, showing that the ice excavated a source of rubble much larger than the altered source of the orange avalanche deposit. For several kilometers, the canyon-marginal moraine bounds a paleovalley filled to 30- to 50-m depth by the avalanche deposit, showing that the narrow Juhle Fork valley glacier had receded considerably before the avalanche took place. The observation that the narrow intracanyon moraine is inset against the older Knife Peak avalanche deposit (the surface of which is unglaciated) supports the evidence previously discussed that valley glaciers occupied the lower Knife Creek valley well into the early Holocene. It remains ambiguous, however, whether the ice tongue then on the floor of the Juhle Fork or the larger Knife Creek valley glacier that still extended to Three Forks represented early Holocene readvances or simply recessional stillstands that belonged to a discontinuous Pleistocene-ending withdrawal which itself persisted into the early Holocene.

Ikagluik Creek Debris-Avalanche Deposit

On the north apron of Mount Griggs, another pinkish-orange debris-avalanche deposit extends from the snout of the north-northwestern glacier to the canyon rim of Ikagluik Creek (unit di, fig. 4). As preserved today, the deposit covers an area of about 3.5 km^2, but because the avalanche filled and laterally overspilled a gorge tributary to Ikagluik Creek, a large additional fraction was evidently reworked downstream as alluvium. Along the tributary gorge, which has reincised the deposit down to Jurassic basement, the poorly sorted avalanche deposit is 20 to 30 m thick, and on the gently sloping plateau adjacent to the gorge it is generally 10 to 15 m thick and topped by numerous mounds and hummocks. Many such mounds are shattered blocks of monolithologic andesite that have disintegrated into piles as much as 3 m high and 15 m wide. Others are lithologically composite, and many 1-m blocks are acid altered, but all are (or were) andesitic. The largest coherent andesite block seen was 5 m across. Two chemically analyzed blocks contain 59 to 60 weight percent SiO_2, and some are unusually rich (for Mount Griggs) in fine-grained mafic enclaves. The fines-bearing matrix is generally pale orange or pink, owing in part to comminution of friable clasts of hydrothermally altered material that can also be white or pale yellow but are commonly laced with orange-brown fracture fillings and crusts.

The avalanche came down over the north-northwestern glacier, probably from its steep-walled cirque (now ice filled) at about 6,000-ft (1,830 m) elevation. Its source was not at the summit because the amphitheater rim on this side is unbroken. For 2 km downstream from the snout of the glacier, orange-colored rubble is reworked as till along the trough, whereas Neoglacial lateral moraines adjacent to the trough are dark gray brown (consisting mostly of unaltered andesite).

The gently sloping distal surface of the avalanche deposit is directly overlain by an accumulation of eolian silt and soil, as much as 75 cm thick, within which we found three tephra layers. The 8-cm-thick middle tephra layer is constrained by regional data to be about 5,500 ^{14}C years old. Beneath that layer, 24 cm of silt/soil is underlain by a 2-cm-thick layer of fine gray ash that rests only a few millimeters above blocks in the avalanche deposit. Organic-bearing silt directly atop that near-basal ash layer yielded a radiocarbon age of 6,250±190 ^{14}C yr B.P. (Geochron Gx-23623), suggesting that the avalanche took place about 7 ka.

Behavior of Glaciers

Six active glaciers descend the slopes of Mount Griggs. For convenience, we refer to these six radially flowing ice tongues (fig. 4) as the southern, east-northeastern, northeastern, north-northeastern, north-northwestern, and northwestern glaciers. The southern glacier is fed from the amphitheater-enclosed icecap, and the other five glaciers from shallow spoon-shaped cirques high on the steep outer slopes of the cone. All six glaciers are thin, narrow, and much less voluminous than those on nearby Mageik, Katmai, and Snowy Mountain volcanoes, each of which stands on the peninsular drainage divide. The 20th-century termini of five of the Mount Griggs glaciers have lain at 3,000- to 3,800-ft (915–1,160 m) elevation (not far below the break-in-slope from steep cone to gentler apron) but at about 5,000-ft (1,525 m) elevation for the southern glacier. The lower third or so of each glacier remains mantled by 1912 fallout, which has been disrupted and commonly thickened by surface reworking and glacier movement. Generally, however, the upper half to two-thirds of each glacier is active, heavily crevassed, and now free of 1912 pumice cover. Neoglacial till preserved at as low as 2,000-ft (610 m) elevation (fig. 4) shows that the northerly glaciers were 2 to 3 km longer earlier in the Holocene.

Inspection of aerial photographs taken in 1951 and 1987 reveals marked differences in behavior of the six glaciers during that 36-year interval. (We are aware of no measurable changes in terminal positions since 1987, although small ones may have occurred.)

Alone among the six glaciers, the southern glacier is confined to the steep part of the cone and has no terminal lobe of gentler gradient. It is unique in having southerly exposure and in being younger than the other glaciers, having originated in the middle or late Holocene after growth of the inner cone created the annular moat where its icefield source accumulates (figs. 5, 7). Its steep terminal reach is covered by 1912 fallout, as well as by andesitic rubble. Although debris obscures the wasting terminus, the active ice front appears to have receded about 400 m (in plan view), withdrawing from 4,800-ft (1,465 m) elevation in 1951 to about 5,500-ft (1,675 m) elevation by 1987.

Of the five northerly glaciers, two have retreated since 1951, two show little change, and one has advanced slightly. Among them, the easternmost (east-northeastern) glacier exhibits the most negative ice budget for the interval 1951–87. Both of its lower lobes (fig. 4) became stagnant piles of ice-cored debris, and its active ice front receded 800 m, from a low of 3,150-ft (960 m) elevation in 1951 to about 4,500-ft (1,370 m) elevation by 1987.

The adjacent northeastern glacier also retreated, but by less than 100 m in plan view, from 2,950-ft (900 m) elevation in 1951 to about 3,100-ft (945 m) elevation by 1987. Although its distal 300 m or so has thinned and shrunk noticeably, recession of the terminus has probably been minimized by its steep inclination in a narrow gorge (fig. 4).

The bilobate north-northeastern glacier appears to be the healthiest of the Mount Griggs glaciers; both lobes have steep bulging flow fronts at about 3,500 ft (1,065 m) elevation. The terminal position of neither lobe changed appreciably between 1951 and 1987.

The north-northwestern glacier shows apparently contradictory behavior. Its lower 400 m forms a bulging pumice-covered lobe at about 3,700-ft (1,130 m) elevation that actually advanced about 40 m between 1951 and 1987. During the same interval, however, the kilometer-long medial reach of the glacier wasted severely, exposing bedrock knobs and stranding an abundance of supraglacial debris.

Finally, the snout of the northwestern glacier showed little change. Its steep but stagnant, pumice-covered terminus maintained an elevation of about 3,500 ft (1,065 m) between 1951 and 1987.

All six glaciers appear to have either retreated or thinned (or both) during the 36-year interval, with the generally negative ice budget probably reflecting gross climatic influence. The absence of a consistent pattern may simply reflect vagaries imposed by some combination of (1) complex responses to the 1912 pumice mantle, (2) localized effects of bed steepness and roughness on flow behavior, and (3) short-term variations in avalanche-supplied contributions of snow and rubble to mass budgets. More systematic patterns of glacier behavior have been observed nearby at Mageik, Trident, Katmai, and Snowy Mountain volcanoes (Hildreth and others, 2000, 2001).

Discussion

Mount Griggs is a steep stratovolcano marked by fumarolic alteration near its summit, ice in its craters, and glaciers on its flanks. Thus, a new eruptive episode would make the cone susceptible to generation of debris flows and possibly, as during the early Holocene, to triggering of debris avalanches. The volcano lies in uninhabited wilderness, however, and the runout distance is 25 km to Naknek Lake (fig. 1). Hazards posed by such events would principally threaten fish and wildlife resources, summer backpackers, and observers attracted by precursory activity. The USGS' Alaska Volcano Observatory has installed several seismometers near Mount Griggs, and were signs of unrest to be detected, additional instrumental and observational monitoring would be implemented, and the land-management authorities, the media, and the aviation community would be notified. In marked contrast to the nearby volcanic-front centers, the area beneath Mount Griggs is today virtually aseismic (Jolly and McNutt, 1999).

Any volcanic-ash plume, associated even with minor eruptions, poses a potential hazard to aircraft, and both local sightseeing flights and scheduled commercial flights (King Salmon to Kodiak) commonly pass close to Mount Griggs. Although layers of Holocene ash fall from other volcanoes are common in the surrounding area, no ash layers attributable to Mount Griggs itself have been identified away from the edifice. To the contrary, no evidence exists that the typically effusive or spatter-fed eruptions of consistently crystal rich andesitic magma at Mount Griggs are accompanied by particularly explosive activity or dispersal of widespread ash clouds. Although Mount Griggs has been fairly active during the Holocene, its characteristic activity has been notably less explosive than that of its more silicic, tephra-producing neighbors Mageik, Martin, Trident, and, of course, Katmai and Novarupta.

Mount Griggs is older than any of its active neighbors, yet, uniquely among them, it has maintained a stable central conduit system, apparently throughout its 300-k.y. lifetime. Mageik and Katmai Volcanoes are both younger than 100 ka, and although each volcano matches or exceeds Mount Griggs in total eruptive volume, their products have issued from several different vents in the course of constructing compound edifices (Hildreth and Fierstein, 2000; Hildreth and others, 2000). Trident, likewise, has built four discrete but overlapping cones and several flanking lava domes during its 140-k.y. eruptive lifetime. What properties of the magma generation, storage, or transport systems (or of the crystal-rich andesitic magma itself) might account for the relative stability that has permitted construction of the centrally symmetrical volcanic edifice of Mount Griggs?

Are such properties related to the position of Mount Griggs 12 km behind the volcanic line? The unresolved question of why so many, closely spaced andesite-dacite stratovolcanoes are perched single file atop the peninsular drainage divide (fig. 1) in Katmai National Park was addressed by Hildreth and others (2001). Equally interesting, however, is why Mount Griggs stands alone, nearby, so exceptionally.

Several other volcanic vents in this part of the Alaska Peninsula, like Mount Griggs, are well behind the main volcanic line, but none are large active cones. Several glaciated scraps of Pliocene basaltic to dacitic lava cap ridges northwest of Mount Griggs (fig. 4), and probably all were erupted there or nearby. Additionally, five small glaciated volcanoes (mapped by Riehle and others, 1993), likewise basaltic to dacitic, are scattered around the upper Savonoski River basin, 25 to 45 km northeast of Mount Griggs and 11 to 21 km behind (northwest of) the Dennison-Steller-Kukak-Devils Desk reach of the volcanic front (fig. 1). In addition, 90 km southwest of Mount Griggs, a brief phreatomagmatic outburst in 1977 produced the Ukinrek Maars and a sheet of basaltic ejecta at a site 10 km behind (northwest of) the frontal stratovolcano Mount Peulik.

These scattered minor volcanic centers have in common with voluminous Mount Griggs not only positions well behind the volcanic front but also magmatic compositions that suggest contributions from the subducting plate which are proportionately smaller than in eruptive products of the main volcanic line. Products of all the volcanoes here, whether on or behind the main chain, have compositions typical of convergent-margin-arc magmas that reflect a significant slab-derived contribution. Nonetheless, the slab geochemical signature is consistently weaker in Mount Griggs lavas than in those of the volcanic-front centers nearby. In particular, samples from Mount Griggs have lower Ba/Zr, Ba/La, Ba/Ta, and Ba/Th ratios (characteristically elevated in arc magmas) than those from Katmai, Trident, Mageik, Martin, and Novarupta. The inference that the magmas erupted at Mount Griggs thus contain a proportionately larger contribution from the subarc mantle wedge is a topic of continuing investigation.

Acknowledgments

Dave Johnston alerted us to the possibility that Mount Griggs might be worth studying, in the course of a memorable field campaign in the summer of 1979, when we were joined by Terry Keith, Anita Grunder, and Peter Shearer (who took the photograph in fig. 8). On the first author's initial visit to Mount Griggs in 1976, he was joined by Larry Jager and Dan Kosco. Michelle Coombs helped on Mount Griggs in 1997. In 1997 and 1998, helicopter pilots Paul Walters and Bill Springer took us everywhere we wanted to go on and around Mount Griggs. Joel Robinson took the lead in digitally compiling our Katmai geologic map, of which figures 3 and 4 are localized adaptations. We are grateful to James Saburomaru and Forrest McFarland for K-Ar dating at the USGS laboratories in Menlo Park, Calif., and to John Paskievitch for his patience and expertise in arranging field logistics. We thank Kevin Scott and Terry Keith for their reviews of the manuscript and the editors for their labors. For encouraging this study, we are especially grateful to Terry Keith, then at the helm of the Alaska Volcano Observatory.

References Cited

Allen, E.T., and Zies, E.G., 1923, A chemical study of the fumaroles of the Katmai region: National Geographic Society Contributed Technical Papers, Katmai Series, no. 2, p. 75–155.

Bacon, C.R., and Druitt, T.H., 1988, Compositional evolution of the zoned calcalkaline magma chamber of Mount Mazama, Crater Lake, Oregon: Contributions to Mineralogy and Petrology, v. 98, no. 2, p. 224–256.

Coombs, M.L., Eichelberger, J.C., and Rutherford, M.J., 2000, Magma storage and mixing conditions for the 1953–1974 eruptions of Southwest Trident volcano, Katmai National Park, Alaska: Contributions to Mineralogy and Petrology, v. 140, p. 99–118.

Detterman, R.L., Case, J.E., Miller, J.W., Wilson, F.H., and Yount, M.E., 1996, Stratigraphic framework of the Alaska Peninsula: U.S. Geological Survey Bulletin 1969–A, 74 p.

Fenner, C.N., 1926, The Katmai magmatic province: Journal of Geology, v. 35, no. 7, pt. 2, p. 673–772.

Fierstein, Judy, and Hildreth, Wes, 1992, The plinian eruptions of 1912 at Novarupta, Katmai National Park, Alaska: Bulletin of Volcanology, v. 54, no. 8, p. 646–684.

Griggs, R.F., 1922, The Valley of Ten Thousand Smokes: Washington, D.C., National Geographic Society, 340 p.

Higbie, R.G., 1975, The Katmai eruption and the Valley of Ten Thousand Smokes, *in* Oehser, P.H., ed., National Geographic Society research reports, 1890–1954: Washington, D.C., National Geographic Society, p. 141–170.

Hildreth, Wes, 1983, The compositionally zoned eruption of 1912 in the Valley of Ten Thousand Smokes, Katmai National Park, Alaska: Journal of Volcanology and Geothermal Research, v. 18, no. 1–4, p. 1–56.

———1987, New perspectives on the eruption of 1912 in the Valley of Ten Thousand Smokes, Katmai National Park, Alaska: Bulletin of Volcanology, v. 49, no. 5, p. 680–693.

Hildreth, Wes, and Fierstein, Judy, 2000, Katmai volcanic cluster and the great eruption of 1912: Geological Society of America Bulletin, v. 112, no. 10, p. 1594–1620.

Hildreth, Wes, Fierstein, Judy, Lanphere, M.A., and Siems, D.F., 1999, Alagogshak volcano; a Pleistocene andesite-dacite stratovolcano in Katmai National Park, *in* Kelley, K.D., ed., Geologic studies in Alaska by the U.S. Geological Survey, 1997: U.S. Geological Survey Professional Paper 1614, p. 105–113.

———2000, Mount Mageik; a compound stratovolcano in Katmai National Park, *in* Kelley, K.D., and Gough, L.P., eds., Geologic studies in Alaska by the U.S. Geological Survey, 1998: U.S. Geological Survey Professional Paper 1615, p. 23–41.

———2001, Snowy Mountain; a pair of small andesite-dacite stratovolcanoes in Katmai National Park, *in* Gough, L.P., and Wilson, F.H., eds., Geologic Studies in Alaska by the U.S. Geological Survey, 1999: U.S. Geological Survey Professional Paper 1633, p. 13–34.

Hildreth, Wes, and Lanphere, M.A., 1994, Potassium-argon geochronology of a basalt-andesite-dacite arc system; the Mount Adams volcanic field, Cascade Range of southern Washington: Geological Society of America Bulletin, v. 106, no. 11, p. 1413–1429.

Jolly, A.D., and McNutt, S.R., 1999, Seismicity at the volcanoes of Katmai National Park, Alaska; July 1995–December 1997: Journal of Volcanology and Geothermal Research, v. 93, no. 3–4, p. 173–190.

Kosco, D.G., 1981, Characteristics of andesitic to dacitic volcanism at Katmai National Park, Alaska: Berkeley, University of California, Ph.D. thesis, 249 p.

Mann, D.H., and Peteet, D.M., 1994, Extent and timing of the Last Glacial Maximum in southwestern Alaska: Quaternary Research, v. 42, p. 136–148.

Miyashiro, Akiho, 1974, Volcanic rock series in island arcs and active continental margins: American Journal of Science, v. 274, no. 4, p. 321–355.

Muller, E.H., 1952, The glacial geology of the Naknek district, the Bristol Bay region, Alaska: Urbana, University of Illinois, Ph.D. thesis, 98 p.

Muller, E.H., 1953, Northern Alaska Peninsula and eastern Kilbuck Mountains, Alaska, in Péwé, T.L., Wahrhaftig, C.A., Fernald,

A.T., Hopkins, D.M., Karlstrom, T.N.V., Krinsley, D.B., and Muller, E.H., Multiple glaciation in Alaska; a progress report: U.S. Geological Survey Circular 289, p. 2–3.

Muller, E.H., Juhle, R.W., and Coulter, H.W., 1954, Current volcanic activity in Katmai National Monument: Science, v. 119, no. 3088, p. 319–321.

Peacock, M.A., 1931, Classification of igneous rock series: Journal of Geology, v. 39, no. 1, p. 54–67.

Poreda, R.J., and Craig, Harmon, 1989, Helium isotope ratios in circum-Pacific volcanic arcs: Nature, v. 338, no. 6215, p. 473–478.

Riehle, J.R., and Detterman, R.L., 1993, Quaternary geologic map of the Mount Katmai quadrangle and adjacent parts of the Naknek and Afognak quadrangles, Alaska: U.S. Geological Survey Miscellaneous Investigations Series Map I–2032, scale 1:250,000.

Riehle, J.R., Detterman, R.L., Yount, M.E., and Miller, J.W., 1993, Geologic map of the Mount Katmai quadrangle and adjacent parts of the Naknek and Afognak quadrangles, Alaska: U.S. Geological Survey Miscellaneous Investigations Series Map I–2204, scale 1:250,000.

Sheppard, D.S., Janik, C.J., and Keith, T.E.C., 1992, A comparison of gas geochemistry of fumaroles in the 1912 ash-flow sheet and on active stratovolcanoes, Katmai National Park, Alaska: Journal of Volcanology and Geothermal Research, v. 53, no. 1–4, p. 185–197.

Singer, B.S., Dungan, M.A., and Layne, G.D., 1995, Textures and Sr, Ba, Mg, Fe, K, and Ti compositional profiles in volcanic plagioclase; clues to the dynamics of calc-alkaline magma chambers: American Mineralogist, v. 80, no. 7–8, p. 776–798.

Stacey, J.S., Sherrill, N.D., Dalrymple, G.B., Lanphere, M.A., and Carpenter, N.V., 1981, A five-collector system for the simultaneous measurement of argon isotope ratios in a static mass spectrometer: International Journal of Mass Spectrometry & Ion Physics, v. 39, p. 167–180.

Wood, C.A., and Kienle, Jürgen, eds., 1990, Volcanoes of North America: Cambridge, U.K., Cambridge University Press, 354 p.